**This is manuscript is a pre-print and has not yet undergone peer-review. Hence subsequent versions of the manuscript may differ in content. Feedback is welcome – please provide any via email to simon.holford@adelaide.edu.au**

# Preservation and re-exposure of late Palaeozoic glacial rock surfaces through cyclical burial and exhumation: apatite fission track evidence from the Fleurieu Peninsula, southeastern Australia

Simon P. Holford[1], Paul F. Green[2], Ian R. Duddy[2], Richard R. Hillis[1], Steven M. Hill[3] & Martyn S. Stoker[1]

[1]Australian School of Petroleum and Energy Resources, University of Adelaide, SA 5005, Australia (simon.holford@adelaide.edu.au)

[2]Geotrack International Pty Ltd, 37 Melville Road, Brunswick West, Victoria 3055, Australia

[3]Geoscience Australia, Cnr Jerrabomberra Ave and Hindmarsh Drive, Symonston, ACT 2609, Australia

## Abstract

The antiquity of the Australian landscape has long been the subject of debate, with some studies inferring extraordinary longevity ($>10^8$ Myr) for some subaerial landforms dating back to the early Palaeozoic. A number of late Palaeozoic glacial erosion surfaces in the Fleurieu Peninsula, southeastern Australia, provide an opportunity to test the notion of long-term subaerial emergence, and thus tectonic and geomorphic stability, of parts of the Australian continent. Here we present results of apatite fission-track analysis (AFTA) applied to a suite of samples collected from localities where glacial erosion features of early Permian age are developed. Our results indicate that the Neoproterozoic-Lower Palaeozoic metasedimentary rocks and granitic intrusions upon which the glacial rock surfaces generally occur were exhumed to the surface by the latest Carboniferous-earliest Permian, possibly as a far-field response to the intraplate Alice Springs Orogeny. The resulting landscapes were

sculpted by glacial erosive processes. AFTA results suggest that the erosion surfaces and overlying Permian sediments were subsequently heated to between ~60 and 80°C, which we interpret as recording burial by a Permian-Mesozoic sedimentary cover, roughly 1 kilometre in thickness. This interpretation is consistent with existing thermochronological datasets from this region, and also with palynological and geochronological datasets from sediments in offshore Mezozoic-Cenozoic-age basins along the southern Australian margin that indicate substantial recycling of Permian-Cretaceous sediments. AFTA suggests that the exhumation which led to the contemporary exposure of the glacial erosion features probably began during Paleogene, during the initial stages of intraplate deformation that has shaped the Mt Lofty and Flinders Ranges in South Australia. Our findings are consistent with several recent studies, which suggest that burial and exhumation has played a key role in the preservation of Gondwanan geomorphic features in the contemporary Australian landscape.

## 1. Introduction

The antiquity of the Australian landscape has been the subject of long-standing debate (Jutson, 1914; King, 1950; Jennings & Mabbutt, 1967; Davies & Williams, 1978), with a number of studies inferring extraordinary longevity of up to several hundred million years for some subaerial Gondwanan landforms (Stewart et al., 1986; Gale, 1992; Nott, 1995), thus implying extreme tectonic and geomorphic stability coupled with negligible rates of denudation and weathering (Twidale, 1998). The notion of long-term surface preservation of Mesozoic- and Palaeozoic-aged landscape elements across Australia, however, is difficult to reconcile with an emerging body of evidence that documents significant landscape rejuvenation across parts of the continent since the Neogene in response to both plate boundary-controlled intraplate deformation and dynamic topography induced by mantle flow (Sandiford, 2003; Quigley et al., 2010; Holford et al., 2011a; Clark et al., 2012; Czarnota et al., 2014; Lubineicki et al., 2019, 2020).

One possible mechanism by which ancient landforms may be preserved in the contemporary landscape is through their burial beneath a sedimentary cover, followed by subsequent exhumation leading to their re-exposure at the Earth's surface (Hill, 1999; Pillans, 2007; Green et al., 2013; Lidmar-Bergström et al., 2013). This hypothesis has been invoked to explain the preservation of planar, Cambrian-age ridge-tops in the Davenport Range (Belton et al., 2004), early Mesozoic-age regolith and high-level plateau surfaces in the southeastern Australian highlands (Hill, 1999), and weathering imprints dated as Late Carboniferous by palaeomagnetic data in the north of the Yilgarn Craton (Pillans, 2005). In all cases the preservation of these ancient landscape elements is ascribed to their burial by several kilometres of sedimentary section during the Mesozoic, with thermochronological data (e.g. apatite fission track analysis) pointing to subsequent removal of this "now-missing" rock section and exhumation of the ancient landforms occurring since the Late Cretaceous (Hill, 1999; Belton et al., 2004; Weber et al., 2005; Pillans, 2007).

Amongst the best-known ancient geomorphic elements that are preserved in the contemporary Australian landscape are a series of glacial features of assumed Early Permian age, which are exposed on the Fleurieu Peninsula in South Australia (Alley, 1995; Normington et al., 2018; Fig. 1). These features, which include glacial tills, glacially polished and striated rock surfaces, and erratic boulders, developed when the Gondwana supercontinent was at mid-to-high latitudes in the Southern

Hemisphere and was extensively covered by large continental ice sheets (Crowell & Frakes, 1971; Fielding et al., 2008).

The localities on the Fleurieu Peninsula (Fig. 2) provide an ideal opportunity to test the hypothesis that ancient landscape elements can be preserved if buried and then brought back to the surface by exhumation, though to date, few studies have attempted to constrain their post-Permian geological histories. Here we present new apatite fission track analysis (AFTA) data from a series of samples collected from localities around the Fleurieu Peninsula that constrain the post-Permian thermal histories of the glacial rock surfaces, and in some cases of the overlying sedimentary deposits. In all cases our results indicate significant post-Permian heating and subsequent cooling, implying burial of the glacial landforms by roughly 1 kilometre of now-missing section prior to exhumation that began during the Paleogene. Our results support the notion that burial and exhumation is an efficient mechanism for the preservation of Gondwanan land surfaces in the contemporary landscape. They also document a dynamic period of km-scale exhumation during the burgeoning stages of continental separation between Australia and Antarctica that has important implications for Mesozoic and early Cenozoic palaeogeographic reconstructions of eastern Gondwana.

## 2. Geological Setting

The Fleurieu Peninsula is located at the southernmost part of the Mount Lofty Ranges in South Australia (Fig. 2). The Mount Lofty Ranges are a roughly ~N-S to NE-SW-trending upland system (maximum elevation of ~700 m) bordered by low regions that are close to or below sea level (i.e. Gulf St Vincent to the west and the Murray Basin to the east) (Sandiford, 2003). The Mount Lofty Ranges and the contiguous Flinders Ranges to the north combine to form an upland system, some 800 km long, which is also known as the Adelaide Fold Belt (Gibson & Stüwe, 2000). The Adelaide Fold Belt consists of Late Proterozoic and Cambrian metasedimentary sequences and Archean basement that were deformed during the Cambrian–Ordovician Delamerian Orogeny (Jenkins & Sandiford, 1992). It is generally thought that the topography created during Delamerian orogenesis was eroded to low relief by the Late Palaeozoic, based on the widespread occurrence of glacial sediments of presumed latest Carboniferous–Early Permian age (the Cape Jervis Formation) that overlie Cambrian and older sequences (Daily et al., 1974; Normington et al., 2018). The area of glacial sediments and erosive features of latest Carboniferous-Early Permian age that encompasses the locations described in this paper has been termed the Troubridge Basin (Wopfner, 1972). The Troubridge Basin sediments are the remnants of a formerly more extensive Upper Palaeozoic sequence, although some of the thickest successions are now preserved in erosional and tectonic troughs around the Fleurieu Peninsula (Alley et al., 1995; Normington et al., 2018).

Due to the discontinuous nature of these glacigenic sediments and the paucity of fauna and flora preserved within them, dating and correlation of these strata has proven difficult (Alley et al., 1995; Normington et al., 2018). Palynological evidence from an outcrop of the youngest parts of the Cape Jervis Formation at Waterloo Bay on the southern Yorke Peninsula indicate an Asselian or Sakmarian (Early Permian) age, though older sections are undated and may be Late Carboniferous in age (Alley et al., 1995). Fielding et al. (2008) reviewed the character and distribution of Upper Palaeozoic glacial deposits in eastern Australia and identified at least eight discrete glacial intervals (each 1–8 Ma in duration), separated by nonglacial intervals and spanning an interval from the mid-Carboniferous (~327 Ma) to the early Late Permian (~255 Ma) (Metcalfe et al., 2014).

The Mount Lofty Ranges are bound by a series of discrete, curvilinear faults that juxtapose Cambrian or older metasedimentary sequences with Eocene or younger sands, clays and carbonates (Flöttmann & Cockshell, 1996; Sandiford, 2003; Lubineick et al., 2019; Preiss 2019). These Cenozoic sediments unconformably overlie the glacial deposits, and it has been suggested that the ~600 m thick Cenozoic (mid Eocene to mid Miocene, and Pliocene to Holocene age) sequence in the Gulf St Vincent Basin to the west of the Fleurieu Peninsula was deposited in a shallow foreland basin that developed contemporaneously with the Cenozoic uplift of the Mount Lofty Ranges (Flöttmann & Cockshell, 1996). It is generally agreed that this uplift is due to ~E-W-directed shortening driven by plate boundary forces, accommodated by reverse-sense reactivation of the faults that bound the Ranges (Bourman & Lindsay, 1989; Sandiford, 2003; Hillis et al., 2008; Holford et al., 2011a; Lubeniecki et al., 2020) and producing a zone of elevated contemporary topography that mimics the spatial extent of the considerably older fold belt created during Delamerian orogenesis (Gibson & Stüwe, 2000).

## 3. AFTA Methodology

The methodological and analytical aspects of AFTA are well established (e.g. Green et al., 2002; Green & Duddy, 2012). AFTA utilizes radiation damage trails (fission tracks) created by spontaneous fission of $^{238}$U within the crystal lattice of apatite, which is a common detrital mineral in most medium-coarse grained clastic sedimentary rocks and occurs as an accessory phase in plutonic and high grade metamorphic rocks. By counting the number of tracks in a polished and etched grain surface and measuring the uranium content, a fission track age can be calculated, which in the absence of other factors provides a measure of the time over which tracks have accumulated. Fission track lengths form within a narrow range (~16 μm), but are progressively shortened as radiation damage is repaired at a rate that increases with temperature (annealing). Shortening leads to a reduction in the number of tracks that can intersect a polished surface, and above 110°C all damage is repaired and no tracks are preserved. A measured fission track age thus represents a balance between production of tracks and loss by annealing and must be assessed along with track length data.

Extraction of thermal history information from AFTA data begins with construction of a Default Thermal History (DTH), derived from the burial history defined by the preserved sedimentary section and the present-day thermal gradient. For a sedimentary rock, this is the history that would apply if the sample has not been any hotter than the present-day temperature at any time since deposition. For basement samples, a similar approach can be adopted using the age of the oldest overlying sedimentary units. If the DTH can explain the AFTA data, then it is not possible to extract further thermal history information. If the AFTA data show a greater degree of annealing (i.e. fission track age and/or track length reduction) than expected from the DTH, then the sample must have been hotter in the past and information on the magnitude and timing of heating and cooling events can be extracted from the data. All samples analysed in this study show a greater degree of annealing (i.e. fission track age and/or length reduction) than that expected from the DTH, and therefore must have been hotter in the past.

To extract thermal history information from AFTA data, we use a kinetic model that makes full quantitative allowance for the effects of chlorine (Cl) content on fission-track annealing rates (Green and Duddy, 2012). Because maximum palaeotemperatures are the key factor that dominates AFTA data, this technique reveals little information on the thermal history prior to the onset of cooling. Therefore, we do not attempt to constrain the entire thermal history of each sample but focus on the key aspects of the thermal history that control the fission track age and length distribution i.e. the maximum palaeotemperature of each sample, and the time at which cooling from that palaeotemperature began (Green and Duddy, 2020).

By modelling expected AFTA parameters resulting from a range of possible thermal histories, we use maximum likelihood theory similar to that described by Gallagher (1995) to define the range of values of maximum palaeotemperature and the onset of cooling giving predictions that match the measured data within 95% confidence limits. We quote results in terms of 95% confidence limits on the range of paleotemperatures and the time at which cooling began, in up to three episodes (Green and Duddy, 2020). Palaeotemperature estimates derived using this approach usually have an absolute uncertainty (i.e. accuracy, as opposed to precision as indicated by the 95% confidence limits) of better than ±10°C. AFTA can provide constraints on up to three episodes, provided each episode is sufficiently separated in paleotemperature and timing. This is most likely when the first episode involves a maximum palaeotemperature sufficient to totally anneal all tracks (typically >110°C), followed by a subsequent peak around 90- 100°C, which leads to shortening of tracks formed after the initial cooling to a mean length of ~10 μm. Finally, cooling to a low temperature is followed by reheating to ~70°C, sufficient to reduce track lengths formed after the second episode to ~12-13 μm. Further details of the AFTA technique are provided by Green and Duddy (2012, 2020) and Green et al. (2013).

**4. Results**

*4.1. Port Elliot*

A glacially polished surface is exposed on a granite promontory between Knights Beach and Green Bay in Port Elliot on the south coast of the Fleurieu Peninsula (Fig. 3a). The polished surface crops out intermittently over a distance of approximately 30 m, and where best exposed, well preserved striations, grooves and possible crescent-shaped gouges indicate a direction of ice movement from approximately east to west (255°to 260°) (Milnes & Bourman, 1972). The polished surface is developed on an outcrop of the Encounter Bay Granite, a medium- to coarse-grained, biotite granite that forms part of an extensive belt of foliated and non-foliated Lower Palaeozoic granites that occur in southeastern South Australia and southwestern Victoria (Dasch et al., 1971). The Rb-Sr isotope data for total-rock, feldspar and muscovite samples of the uncontaminated inner facies and metasedimentary-contaminated border facies of the Encounter Bay Granite indicate emplacement between 515 ± 8 and 506 ± 6 Ma, during the Late Cambrian (Milnes et al., 1977). Metamorphic assemblages in Kanmantoo Group metasediments intruded by the granites imply emplacement at a depth of less than ~10 km, and possibly as shallow as 5 km (Milnes et al., 1977), with the polished surface at Port Elliot indicating exhumation to the surface by at least the Early Permian. Sediments of presumed Early Permian age overlying the granite are exposed in a small cutting several metres to the north of the best-developed section of the polished surface, and include thinly-bedded glacial silts with minor grit bands that form part of the Cape Jervis Formation (Milnes & Bourman, 1972; Alley et al., 1995).

We collected a sample of the Encounter Bay Granite (GC1069-33) from the fresh surface of a NE-striking joint plane, approximately 20 metres to the southwest of the polished surface. A pooled fission track age of 226.3 ± 10.2 Ma was determined from 20 apatite grains in this sample (Fig. 3b), with a mean fission track length of 12.85 ± 0.11 µm (Fig. 3c). Chlorine is well known to exert a first-order control on fission track annealing in apatite (e.g. Gleadow & Duddy, 1981) and we measured wt% Cl contents in every grain with an electron microprobe. All grains have less than 0.04 wt% Cl, with the exception of one grain containing 0.07 wt% Cl (Fig. 3b). The fission track age is significantly younger than the crystallization age of the granite, and immediately indicates cooling from significant (i.e. >100°C) palaeotemperatures during the Late Palaeozoic or Mesozoic. Thermal history analysis of this sample defines two episodes of heating and cooling. The earliest involves cooling from a maximum palaeotemperature of >103°C some time between 292 and 239 Ma, with the later episode involving cooling from a lower palaeotemperature peak of 62 to 72°C beginning between 76 Ma and the present day (Fig. 3d).

*4.2. Hallett Cove*

Hallett Cove is one of the best known geological sites in Australia because of the evidence for glaciation discovered by Tate (1879), subsequently recognized as being from the Late Palaeozoic by Howchin (1924). Here the glacial deposits of the Cape Jervis Formation unconformably overlie folded Neoproterozoic Brachina Formation psammites (Bourman & Alley, 1990; Normington et al., 2018). Evidence for glacial activity at this site includes numerous, well-preserved glacial erosion features including grooves, striae, friction cracks, polished bedrock (Fig. 4a) and 'p-forms' (irregular, polished and smoothed bedrock surfaces eroded by ice and subglacial meltwater) (Alley et al., 1995). Although the striae vary in orientation, and typically exhibit cross-cutting relationships, the direction of ice movement is inferred to be approximately northwesterly (Bourman & Alley, 1990). The glacigenic sedimentary facies include a lodgement till indicative of glacial advance and developed contemporaneously with the glacial and subglacial meltwater erosion features, and a subaquatic flow till complex and glaciolacustrine sediments that were deposited as the ice sheet stagnated (Bourman & Alley, 1990). Palynomorph data are only available for the lodgement till deposits and form a restricted assemblage lacking age-diagnostic features, and hence the stratigraphic context of the glacigenic deposits at Hallett Cove is not constrained beyond Early Permian (Bourman & Alley, 1990).

We analysed two samples for fission track analysis at Hallett Cove (Fig. 4b). Sample GC1069-66 is a medium-grained glaciolacustrine sand of presumed Early Permian age from Sugarloaf Creek, and sample GC1069-67 is a fine-grained sandstone obtained from an outcrop of the Ediacaran Brachina Formation on a wave-cut platform beneath Black Cliff.

Sample GC1069-66 gave a pooled fission track age of 398.9 ± 19.7 Ma based on 20 grains (Fig. 4c) and a mean fission track length of 12.77 ± 0.13 μm (Fig. 4d). The majority of apatite grains contained <0.05 wt% Cl, with the remaining grains exhibiting a range of contents from 0.07 to 0.74 wt% Cl (Fig. 4c). The fission track age is considerably older than the depositional age of the sample and implies that post-depositional heating was not of sufficient magnitude to produce significant age reduction in the detrital apatite grains within the sample. This is confirmed by our thermal history analysis, which constrains one rather poorly defined period of post-depositional heating and cooling, from a maximum palaeotemperature peak of 63 to 76°C beginning between 136 Ma and 12 Ma (Fig. 4e). There is evidence for two periods of heating and cooling prior to the deposition of the sample. The earliest of these is from a palaeotemperature of >130°C beginning between 651 and 454 Ma, with the second involving cooling from a palaeotemperature of between 86 and 116°C at some time between 498 and 320 Ma.

For sample GC1069-67 a pooled fission track age of 252 ± 15.6 Ma was determined based on 20 apatite grains (Fig. 4f) with a mean fission track length of 12.12 ± 0.16 µm (Fig. 4g) and wt% Cl contents mostly <0.18. Thermal history analysis of this sample defines three episodes of heating and cooling (Fig. 4h). The earliest episode involves cooling from a palaeotemperature peak of >110°C before 300 Ma. This is followed by a subsequent episode of cooling from a lower palaeotemperature peak of 91 to 103°C beginning some time between 315 and 204 Ma, with a final episode involving cooling from a palaeotemperature peak of 67 to 77°C between 56 and 6 Ma. This is interpreted to represent the same palaeothermal episode as the poorly resolved post-depositional episode observed in sample GC1069-66.

### *4.3. Cape Jervis*

This locality hosts the type section of the Cape Jervis Formation (Alley & Bourman, 1984; Bourman & Alley, 1990; Normington et al., 2018). To the north of the Cape Jervis lighthouse (Fig. 5a), glacigenic deposits of presumed Lower Permian age unconformably overlie Lower Cambrian metasandstones belonging to the Carrickalinga Head Formation (Kanmantoo Group), forming cliffs up to 30 m high

(Alley & Bourman, 1984; Normington et al., 2018). The top of the Carrickalinga Head Formation is marked by a fractured layer, ca. 0.5 m thick, interpreted to be the result of frost-shattering (Alley et al., 1995), though no diagnostic sub-glacial erosion features such as striae have been documented from this site. The glacigenic sequence at Cape Jervis is approximately 40 m thick and exhibits significant lithological variability that show a range of subglacial and postglacial environments (Alley et al., 1995). A restricted arenaceous marine foraminiferal assemblage from the shallowest, silt- and clay-dominated unit at the type section indicates a Sakmarian age (Alley et al., 1995).

We collected two samples from this locality. Sample GC1069-68 is a sandstone from an interstratified section of the Permian sequence approximately 10 m above the unconformity, and sample GC1069-69 is a Lower Cambrian metasandstone from an exposure approximately 10 m below the unconformity (Fig. 5a). Sample GC1069-68 was collected in order to evaluate the degree to which the Permian section had been more deeply buried, whilst sample GC1069-69 was collected to show the time when the metasediments were initially exhumed to the surface.

The Lower Permian sample GC1069-68 yielded a pooled fission track age of 339.5 ± 17.8 Ma from 20 apatite grains containing between 0.00 and 0.65 wt% Cl (Fig. 5b), together with a mean fission track length of 11.61 ± 0.22 μm (Fig. 5c). The thermal history results for this sample are similar to those for the Permian sample GC1069-66 from Hallett Cove. Thermal history analysis defined one pre-depositional and one post-depositional episode of heating and cooling, plus an intermediate episode that overlaps the timing of deposition (Fig. 5d). The pre-depositional episode involves cooling from a palaeotemperature peak of >130°C beginning between 582 and 443 Ma. The intermediate episode is characterized by cooling from a palaeotemperature range of 95 to 100°C between 380 and 244 Ma. The post-depositional cooling episode is from a palaeotemperature range of 71 to 80°C beginning sometime between 73 and 8 Ma. Assuming that this sample experienced a similar history to sample GC1069-69 (discussed below) allows the constraints on the most recent episode of heating and cooling at this location to be further refined to cooling from a palaeotemperature of 71 to 75°C beginning between 50 and 8 Ma.

The Lower Cambrian sample GC1069-69 gave a pooled fission track age of 260.6 ± 14.1 Ma from 20 apatite grains with wt% Cl contents of ≤0.01 (Fig. 5e), with a mean fission track length of 12.23 ± 0.15 μm (Fig. 5f). Thermal history analysis of this sample revealed three palaeothermal events (Fig. 5g). The earliest episode of cooling is from a palaeotemperature peak of >130°C beginning some time before 307 Ma. This is followed by a subsequent episode of cooling from a lower palaeotemperature range of 92 to 103°C beginning some time between 317 Ma and 211 Ma. The final episode of cooling is from a palaeotemperature range of 65 to 75°C beginning between 50 Ma and the present-day.

*4.4. Inman Valley*

The township of Inman Valley contains a classic geological locality that led Selwyn (1860) to record the first evidence from South Australia for the widespread glaciation of Gondwana during the Late Palaeozoic. In the bed of the Inman River there is an outcrop of Lower Cambrian Kanmantoo Group (Backstairs Passage Formation) metasedimentary rocks marked by a glacially striated, grooved and polished bedrock surface (Fig. 6a). This outcrop is now a geological monument that is commonly referred to as 'Selwyn Rock' or 'Glacier Rock' (Alley, 1995). The southern bank of the Inman River is formed by a sequence of ?Permian glacial deposits that unconformably overlies the Kanmantoo Group and contains a large erratic of the Encounter Bay granite.

We collected a metasandstone sample (GC1069-70) from an outcrop of the Kanmantoo Group from beneath the Permian glacial strata (Fig. 6a). Though the outcrop we sampled did not contain any diagnostic subglacial features, we infer that it experienced a similar post-Permian geological history to the polished bedrock surface based on its close proximity (several metres). This sample gave a pooled fission track age of 260 ± 16.1 Ma based on 19 apatite grains containing between 0.02 and 0.10 wt% Cl (Fig. 6b), with a mean track length of 11.94 ± 0.20 μm (Fig. 6c). Our thermal history analysis of this sample defines three episodes of heating and cooling (Fig. 6d). The earliest episode involves cooling from a maximum palaeotemperature of >110°C some time between 504 and 317 Ma. The intermediate episode is characterized by cooling from a palaeotemperature peak of 90 and 100°C between 279 and 158 Ma. The latest cooling episode is from a lower palaeotemperature peak of 60 to 70°C beginning between 78 and 0 Ma.

### *4.5. Rosetta Head (The Bluff), Victor Harbor*

Rosetta Head (The Bluff) is a prominent landform located ca. 5 km to the southwest of Victor Harbor. It is comprises an outcrop of the Encounter Bay Granite intruding the Kanmantoo Group (Milnes et al., 1977). The smooth, rounded profile of Rosetta Head has been described by some workers as an example of a roche moutonnée, and thus directly related to the passage of an overlying glacier, though no direct evidence for glacial activity has been reported from this locality (Bourman & Milnes, 1977). A sample of medium-grained megacrystic granite (GC1069-71) was collected from this locality to provide additional constraints on the exhumation history of the Encounter Bay Granite suite.

A pooled fission track age of 273.1 ± 12.5 Ma was determined for this sample from 20 apatite grains containing <0.04 wt% Cl (Fig. 7a), with a mean fission track length of 11.89 ± 0.15 μm (Fig. 7b). Thermal history analysis of this sample revealed three episodes of heating and cooling (Fig. 7c). The earliest episode involves cooling from a palaeotemperature peak of >120°C beginning sometime between 372 and 322 Ma. The intermediate episode involves cooling from a palaeotemperature range of 90 to 100°C beginning sometime between 301 and 112 Ma. The final episode of cooling is from a palaeotemperature of 60 to 77°C beginning sometime between 47 and 0 Ma.

*4.6 Sellicks Hill*

The ~NE-SW striking Willunga Fault is one of the most prominent neotectonic structures in southeastern Australia (Sandiford, 2003). The fault is characterized by a distinctive scarp with elevation up to 400 m, which juxtaposes the downthrown Willunga Embayment (containing Cenozoic strata) from the upthrown Sellicks Hill (composed of Cambrian and Neoproterozoic metasedimentary rocks) (Sandiford, 2003; Lubiniecki et al., 2019; Preiss, 2019). The most proximal occurrences of Permian sedimentary rocks are found several km to the southeast of Sellicks Hill in the Myponga Basin, where groundwater wells indicate that Permian strata reach a thickness of ~300 m (Barnett & Rix, 2006). The Permian strata in the Myponga Basin are unconformably overlain by Middle Miocene limestones (Pledge et al., 2015). It has been argued that the Willunga Fault originally formed during the mid Eocene as a bounding fault to a NNW-SSE oriented half-graben (Flöttmann & Cockshell, 1996), though Preiss (2019) has recently argued for a more complicated history, with initiation of the fault in the Early Cambrian and multiple phases of extensional and compressional reactivation during the Palaeozoic and Mesozoic. It is generally agreed that the Willunga Fault has experienced dominantly reverse reactivation since the mid-Cenozoic (Sandiford, 2003; Preiss, 2019) with post-Early Miocene displacement estimated at ~240 m (Tokarev et al., 1999).

A coarse-grained arkose sample (GC545-2) of the Cambrian Mount Terrible Formation was collected at a roadside cutting along Main South Road. The sample is situated in the hangingwall of the Willunga Fault, approximately 1.5 km south of an exposure of the fault in Cactus Canyon (Holford et al., 2011b). A central fission track age of 238.6 ± 18.3 Ma was determined for this sample from 20 apatite grains containing <0.2 wt% Cl (Fig. 8a), with a mean fission track length of 12.56 ± 0.14 μm (Fig. 8b). Thermal history analysis of this sample revealed two episodes of heating and cooling (Fig. 8c). The earliest episode involved cooling from a paleotemperature peak of >103°C beginning sometime between 334 and 248 Ma. The latest episode of cooling is from a palaeotemperature of 71 to 78°C beginning sometime between 94 and 26 Ma.

### *4.7 Myponga Beach*

To obtain additional insights into the exhumation history in the hangingwall of the Willunga Fault, we analysed two siliciclastic samples of the Lower Cambrian Sellick Hill Formation collected at Myponga Beach, ~7 km to the WSW of the road cutting where GC545-2 was collected (Section 4.6). The Myponga Beach samples were collected ~10 km to the south and east of the interpreted offshore trace of the Willunga Fault (c.f. Preiss, 2019). Based on geological mapping and four measured stratigraphic sections at Myponga Beach, Alexander & Gravestock (1990) identified five facies associations within the Sellicks Hill Formation. GC545-3 was collected from the base of Section 5 (Facies A), and GC545-4 was collected from the base of Section 4 (Facies B).

A central fission track age of 271.7 ± 20.2 Ma was determined for sample GC545-3 based on the analysis of 20 apatite grains containing <0.6 wt% Cl (Fig. 9a), with a mean fission track length of 12.61± 0.15 μm (Fig. 9b). Thermal history analysis of this sample revealed two episodes of heating and cooling (Fig. 9c). The earliest episode involved cooling from a paleotemperature peak of between 107 and 117°C beginning sometime between 364 and 264 Ma. The latest episode of cooling is from a palaeotemperature of 65 to 74°C beginning sometime between 60 and 0 Ma.

A pooled fission track age of 284.4 ± 18.1 Ma was determined for sample GC545-4 based on the analysis of 20 apatite grains containing <0.5 wt% Cl (Fig. 9d), with a mean fission track length of 12.61± 0.14 μm (Fig. 9e). Thermal history analysis of this sample revealed two episodes of heating and cooling (Fig. 9f). The earliest episode involved cooling from a paleotemperature peak of >113°C beginning sometime between 370 and 298 Ma. The latest episode of cooling is from a palaeotemperature of 64 to 77°C beginning sometime between 93 and 18 Ma.

## 5. Discussion

The major finding of this study is that both glaciated bedrock features of presumed Early Permian age and overlying Permian glacial sediments at various localities around the Fleurieu Peninsula in southeastern Australia have been significantly hotter than present-day temperatures in post-Permian time Our results thus provide compelling support for the notion that burial and exhumation has played a key role in the survival of ancient, Gondwanan geomorphic features in the contemporary Australian landscape. Following a regional synthesis of our AFTA results, the ensuing discussion focuses on two key questions: firstly, when were the bedrock surfaces upon which the glacial features are developed initially exhumed to the surface? And secondly, by what thickness of cover have they been buried subsequent to their most recent exhumation?

*5.1. Synthesis and discussion of results*

Our results reveal three dominant palaeothermal episodes, which are observed in the majority of the AFTA samples (Fig. 10). Most of the Neoproterozoic and Cambrian samples we collected provide evidence for one or two stages of Late Palaeozoic– early Mesozoic cooling from palaeotemperatures of >86°C, whilst all samples we analysed, including those from outcrops of late Palaeozoic-age glacigenic sediments, provide evidence for cooling from palaeotemperatures of the order of 60 to 80°C beginning during the Late Cretaceous or Cenozoic. Furthermore, the two samples of Late Palaeozoic-age glacial sediments provide evidence for a pre-depositional cooling episode from palaeotemperatures >130°C during the late Neoproterozoic to Early Palaeozoic. In the absence of any significant igneous activity, or evidence for conductive heating by hydrothermal fluids in our study area over the past ~300 Myr, we consider it likely that much of the observed heating and cooling is principally related to the deeper burial (with peak burial depths occurring around the time of peak palaeotemperatures) and subsequent exhumation of the apatite grains analysed in our samples. This interpretation is consistent with regional fission track studies, which suggest that large tracts of southern and southeastern Australia have been exhumed by several kilometres since the Late Palaeozoic (Gibson & Stüwe, 2000; Gleadow et al., 2002; Kohn et al., 2002; Boone et al., 2016; Hall et al., 2016).

*5.1.1. Late Neoproterozoic–Early Palaeozoic cooling*

We interpret the earliest cooling episode identified in this study, which is recorded by detrital apatites that have been recycled into the two glacigenic samples of assumed Permian age, as recording the initial period of exhumation of Neoproterozoic and Lower Cambrian metasediments in the Fleurieu Peninsula. In both samples, this event is characterized by cooling from palaeotemperatures exceeding 130°C. Combining the individual timing constraints from these samples suggests an onset of cooling beginning between 582 and 454 Ma (Fig. 10). The youngest preserved Lower Palaeozoic sedimentary rocks in the Fleurieu Peninsula belong to the Middle Cambrian Kanmantoo Group (Gravestock, 1995), though Milnes et al. (1977) have suggested that at least 5 km of additional sedimentary section may have existed above the Kanmanatoo Group to account for the observed metamorphic grade. The Cambrian and Neoproterozoic sequences were deformed during the Delamerian Orogeny, which is believed have commenced around ~514 Ma and terminated by ~490 Ma (Foden et al., 2006), though some workers have presented geochronological evidence to suggest an earlier onset of deformation (~554 Ma), prior to the deposition of the Kanmantoo Group (Turner et al., 2009). Our favoured interpretation is that this Late Neoproterozoic-Early Palaeozoic cooling episode identified in this study represents uplift and exhumation associated with the termination of the Delamerian Orogeny.

*5.1.2. Late Palaeozoic cooling*

Our results define two periods of cooling during the Late Palaeozoic–early Mesozoic (Fig. 10). The earliest of these is observed in all samples except for GC1069-33 (from Port Elliot), and is characterized by cooling from palaeotemperatures ranging from between 86 to 116°C (sample GC1069-66 from Hallett Cove) and >130°C (sample GC1069-69 from Cape Jervis). In sample GC1069-70 (from Inman Valley), the timing of cooling (beginning between 504 and 317 Ma) overlaps with the earlier cooling episode described in Section 5.1.1, though combining the individual timing constraints from all samples leads us to conclude that this represents a distinct cooling episode that commenced between 334 and 322 Ma.

We identify a subsequent cooling episode that is recorded in four AFTA samples (GC1069-33, 67, 69 and 71) which we interpret to represent the final stage of exhumation leading to the surface exposure of the Neoproterozoic and Cambrian metasediments and granitic intrusions, upon which the glacial erosion features are developed at various locations around the Fleurieu Peninsula. The constraints on the timing of this episode are broadly similar for samples GC1069-67 from Hallett Cove (beginning between 315 and 204 Ma), GC1069-69 from Cape Jervis (beginning between 317 and 211 Ma) and GC1069-71 from Victor Harbor (beginning between 301 and 112 Ma).

As described above, precise constraints on the timing of Late Palaeozoic glaciation events across the Fleurieu Peninsula are broad because of a paucity of robust biostratigraphic data. Restricted foraminiferal assemblages from the type locality of the Cape Jervis Formation indicate a Sakmarian age (295.0 to 290.1 Ma) for the uppermost, marine-influenced unit (Alley et al., 1995). The Lower Cambrian, metasedimentary sample we analysed from this location (GC1069-69) required cooling from a palaeotemperature of 92 and 103°C beginning some time between 317 and 211 Ma in order to explain the observed AFTA parameters (Fig. 4g). Whilst this allows the possibility of cooling having occurred subsequent to the deposition of the glacigenic section at this locality, the Permian-age sample GC1069-68 does not show this episode, instead cooling from a maximum post-depositional palaeotemperature of 71 to 80°C beginning between 73 and 8 Ma (Fig. 4d). We thus interpret the results from GC1069-69 as recording the exhumation of the Kanmantoo Group metasediments to surface levels during the Carboniferous-earliest Permian, prior to development of the glacial landscape features. We infer a similar history for the Neoproterozoic metasediments at Hallett Cove, upon which the glacial erosion features are developed, with AFTA sample GC1069-67 recording cooling from a palaeotemperature peak of 91 to 103°C beginning between 315 and 204 Ma.

The sample of Upper Cambrian Encounter Bay Granite (GC1069-33) we collected from a joint plane close to the polished glacial surface at Port Elliot exhibits a similar thermal history style to the Lower Palaeozoic and Neoproterozoic samples from Cape Jervis and Hallett Cove, with cooling from a maximum palaeotemperature peak during the Late Palaeozoic, followed by a subsequent period of cooling during the late Mesozoic–Cenozoic (Fig. 3d). Interpretation of the early cooling episode is not straightforward, because analysis indicates cooling from a maximum palaeotemperature of >103°C beginning between 292 and 239 Ma i.e. after the Sakmarian, when the Cape Jarvis Formation is thought to have been deposited. This episode could be interpreted as recording rapid burial of the polished glacial surface by a thick (probably >3 km) Permian section, with exhumation beginning shortly after peak burial conditions (Scenario 2 in Fig. 3d). We do not think that this scenario is likely; though we were not able to sample the Cape Jervis Formation at Port Elliot, our samples from Cape Jervis and Hallett Cove indicate maximum post-depositional palaeotemperatures of 71-80°C and 63-76°C for the glacigenic sediments at these respective localities.

Our preferred interpretation is that this early episode represents the rapid exhumation of the Encounter Bay Granite prior to the development of the polished surface (Scenario 1 in Fig. 3d), with AFTA defining the onset of cooling from >110°C as beginning some time between 292 and 239 Ma. Furthermore, the general consistency between the results from this sample, and those from Cape Jervis and Hallett Cove supports an interpretation of this event in all samples in terms of exhumation immediately prior to glaciation. Evidently, some direct biostratigraphic constraints on the age of the Permian section at Port Elliot, coupled with additional thermochronological analysis of Encounter Bay Granite samples from this location are desirable if the pre-glacial exhumation history of the polished surface is to be more fully understood. One possible implication of the interpretation of our results is that the age of the glacigenic sediments of the Cape Jervis Formation in the Fleurieu Peninsula, which have been approximately constrained as Asselian–Sakmarian, may be somewhat younger than hitherto thought.

Assuming that the Late Palaeozoic–early Mesozoic cooling episodes recorded by samples GC1069-33, 67, 69 and 71 represent the same event, a consistent onset of cooling beginning between 292 and 239 Ma is defined (Fig. 10). We note that our interpretation of the AFTA results, which indicates two periods of Late Palaeozoic cooling beginning between 334 and 322 Ma, and 292 and 239 Ma, is broadly consistent with the earlier AFTA investigation by Gibson & Stüwe (2000), which was conducted just to the north of our study area. Gibson & Stüwe (2000) reported that selected AFTA samples from the Mount Lofty Ranges exhibit evidence for cooling from palaeotemperatures >120°C beginning prior to 350 Ma, and from ~95 to 115°C during a subsequent event beginning between 300 and 270 Ma. The likely causes of these cooling episodes are discussed later in this paper.

*5.1.2. Early-mid Mesozoic cooling?*

One of the samples we analysed (GC1069-70 from Inman Valley) provided evidence for a distinct cooling episode from a well-defined palaeotemperature peak of 90 to 100°C beginning between 279 and 158 Ma (i.e. during the Mid-Permian to the Late Jurassic; Fig. 6d). In contrast to sample GC1069-69 from Cape Jervis, which records the exhumation of the Kanmantoo Group prior to Permian glaciation and sedimentation, it is possible that the results from GC1069-70 record the reburial of the glaciated, polished bedrock surface by thick Permian (and possibly Triassic and Jurassic) sediments. This cooling episode appears to be restricted to the Inman Valley and is not recorded by the samples of the Cape Jervis Formation that we collected from the type locality and Hallett Cove. The restriction of this episode to Inman Valley may reflect the locally thicker accumulation of Permian section here, with the recorded thickness of Permian sediments in the Inman Valley region exceeding 300 m but potentially being much thicker (Crowell & Frakes, 1971).

An alternative interpretation of this episode is that it reflects the same Permian to Mid-Triassic (292–239 Ma) event that is observed in samples from Hallett Cove, Cape Jervis, Rosetta Head and Port Elliot. The magnitude of the palaeotemperature peak (~90-100°C) is very similar to that in the other samples that show this event, though assuming that GC1069-70 records the same cooling episode would suggest a later onset of cooling across the region, beginning between 279 and 239 Ma. This would imply an even younger age (Mid–Late Permian?) for glacial activity in this area, which we think is probably unlikely. A further possibility is that this episode records localized heating by hot fluids, presumably through permeable units within the Permian strata or at the unconformity between the Cambrian metasediments and the Permian section. A further alternative explanation for the apparently later cooling in sample GC1069-70 is that the timing constraint could simply represent a statistical outlier from the 292-239 Ma cooling episode, since with 20 individual estimates of the onset of cooling, one might reasonably be expected to fall outside 95% confidence limits. On balance, this option represents our preferred interpretation.

*5.1.3. Paleogene cooling*

All samples analysed in this study record evidence from cooling of palaeotemperatures in the region of 60 to 80°C beginning during the Cretaceous or Cenozoic (Fig. 11). In some samples (e.g. GC1069-66 from Hallett Cove) the constraints on the onset of this cooling are quite broad (beginning between 136 and 12 Ma) whilst in other samples the onset of cooling is more precisely defined (e.g. GC1069-69 from Cape Jervis which began cooling between 50 and 0 Ma). Whilst no known Cretaceous rocks occur within this study area, Cenozoic marine and non-marine units are variably preserved in marginal basins that flank and occur within the Mt Lofty Ranges (Lindsay & Alley, 1995; Pledge et al., 2015). These units help place some additional constraints on the probable time of exhumation associated with this cooling episode. Hallett Cove is situated in the hangingwall of the Eden-Burnside Fault, where there is considerable evidence for Cenozoic displacement (Bourman & Lindsay, 1989; Sandiford, 2003; Clark et al., 2012). At this location the Cape Jervis Formation is unconformably overlain by the Upper Pliocene Hallett Cove Sandstone, a one-meter-thick, transgressive, shallow marginal marine calcareous sandstone to sandy limestone (Lindsay & Alley, 1995). Hence at this location the Permian section must have been exhumed to the surface by the Late Pliocene, consistent with results from sample GC1069-66 that indicate that the second phase of cooling recorded by the sample of the Brachina Formation had begun by at least 12 Ma.

Combining timing constraints for all samples suggests that cooling began between 47 and 26 Ma (Fig.10). Using a present-day surface temperature of 20°C, and applying an arbitrary palaeogeothermal gradient of 30°C $km^{-1}$ implies that samples that crop out throughout our study area were buried by more than ~1 km of Permian to Paleogene section prior to the onset of cooling in this episode. If exhumation occurred rapidly, and advective heating raised geothermal gradients at shallow crustal levels, or if the thermal conductivity of the removed section was low, the amount of required section to be eroded would be reduced. Some evidence for this notion is provided by constraints on subsurface temperatures acquired during the drilling of the Stansbury West-1 well on the Yorke Peninsula in 1966 (Fig. 12). This well encountered ~303 m of ?Permian-aged sedimentary rocks, overlying ~1.4 km of Cambrian and older strata. Subsurface temperatures were measured during a series of drill-stem tests (DSTs) conducted at various depths within the well. When the DST temperatures are plotted against depth (Fig. 12), they reveal evidence for a non-linear geothermal gradient, with the ?Permian sequence characterised by a higher geothermal gradient (46.2°C $km^{-1}$ assuming a present-day surface temperature of 21°C), and the Cambrian and older strata characterised by a lower geothermal gradient (24.7°C $km^{-1}$). These data indicate that the thermal conductivity of preserved Permian sedimentary rocks is considerably lower than that of underlying Cambrian and older sequences.

### *5.2. Tectonic and palaeogeographic implications*

#### *5.2.1. Late Palaeozoic*

Our AFTA results imply that Lower Palaeozoic and Neoproterozoic metasedimentary rocks and granitic intrusions at several locations around the Fleurieu

Peninsula in southeastern Australia were exhumed to the surface prior to or during the Early Permian glaciation of Gondwana, from burial depths of up to 3 km. Previous workers (e.g. Milnes & Bourman, 1972) have suggested that much of this exhumation may have been accomplished during and by the glacial activity, but we note that a significant Late Palaeozoic exhumation event is observed throughout much of southern Australia. In a study conducted immediately to the north of our study area, Gibson & Stüwe (2000) presented AFTA results from a suite of samples collected from outcrops across the Mount Lofty Ranges that cooled from palaeotemperatures of >120°C before 350 Ma, and from around 95-115°C beginning between 300 and 270 Ma. Further to the north, Mitchell et al. (2002) described an extensive suite of apatite fission track data from the northwestern Curnamona Craton and northernmost Flinders Ranges that indicated variable but regional cooling of these areas from palaeotemperatures of >110°C during the Late Carboniferous to Early Permian (commencing between ~310 to 260 Ma). To the northwest of our study area, Tingate & Duddy (2002) report Carboniferous-Permian cooling (350 to 250 Ma) in AFTA samples from several wells in the Officer Basin and Hall et al. (2016) report rapid late Carboniferous-early Permian cooling in apatite fission track data from the Peake and Denison Inliers in northern South Australia. A regional compilation of AFTA and organic maturity data from several basins (the Amadeus, southern Georgina, Perdika and Simpson Desert) located in central Australia also documents widespread cooling, broadly commencing during the Late Carboniferous to Early Permian (Gibson et al., 2005). In all these studies, the authors interpret this cooling in terms of exhumation related to the proximal or distal effects of the Alice Springs Orogeny, which was characterized by a distinct episodic temporal evolution (cf. Shaw et al., 1991; Haines et al., 2001; Raimondo et al., 2014). Our results provide further support for the notion of widespread exhumation across southern Australia during the latest Carboniferous-earliest Permian. Glacial erosive processes may have accentuated this exhumation, but we suggest that the regional extent of this exhumation points to a driving mechanism that is primarily tectonic in origin.

*5.2.2. Permian-Mesozoic*

Following the development of the glacial surfaces of presumed Early Permian age, our AFTA results indicate that these features underwent variable but significant burial. Deeper burial at Inman Valley may have culminated by the Late Jurassic, although AFTA results from the other sites we have sampled imply that maximum post-Permian burial depths occurred by the Late Cretaceous or Paleogene. We speculate that a significant component of this now-removed section across the region comprised Permian sediments. The maximum known thickness of Permian sediments in the Fleurieu Peninsula is ~300 m in Back Valley, to the south of Inman Valley (Alley & Bourman, 1995). To the west of the Fleurieu Peninsula, 339 m of sedimentary rocks assigned to the Cape Jervis Formation were penetrated by the Enchilada-1 well drilled in Gulf St Vincent, similar to the 303 m of presumed Permian-age strata encountered by Stansbury West-1 on the Yorke Peninsula. To the east of the Fleurieu Peninsula, the Donna-1 petroleum exploration well encountered at least 167 m, but possibly as much as 549 m of Cape Jervis Formation sediments (Brakel & Totterdell, 1995). However, seismic reflection data acquired to the south of the Fleurieu Peninsula (Fig. 2) suggests the existence of up to ~2 km of Permian section in a trough incised into underlying Lower Palaeozoic crystalline and metasedimentary rocks (Flöttmann & Cockshell, 1996). This Permian section is in turn overlain by up to 1 km of Cenozoic section (Alley & Bourman, 1995). This section is yet to be tested by drilling, but if the interpretation of Flöttman & Cockshell (1996) is correct, this implies that the preserved offshore Permian sequence is comparable in thickness to the degree of burial of the Permian glacial surfaces and sediments onshore as suggested by our AFTA results.

Further support for the existence of a thick cover of Permian strata across parts of the Fleurieu Peninsula is provided by the occurrence of abundant reworked Permian palynomorphs in Cretaceous siliciclastic rift and post-rift successions in the Ceduna and Duntroon (Alley and Clarke, 1992) and Otway basins (Duddy, 2003) to the southwest and southeast of the Fleurieu Peninsula, respectively. A dredge sample of the Maastrichtian-early Danian Potoroo Formation, obtained from the Duntroon Sub-basin about 150 km west of Kangaroo Island, contained palynomorphs indicative of Kungurian (283.5 to 272.3 Ma) or younger Permian assemblages (Alley & Clarke, 1992). Sediments of this age are not known from proximal Permian basins including those around the Fleurieu Peninsula, with the nearest Kungurian or younger Permian sediments found in small Permian-Triassic Springfield Basin in the southern Flinders Ranges, approximately 600 km to the northeast of the dredge site. Alley & Clarke (1992) thought it unlikely that the recycled palynomorphs were derived from this location, suggesting that the source was more probably a now eroded unit from the proximal Permian basins (including the Troubridge Basin), or perhaps much more distant (e.g. the Cooper Basin in northeastern South Australia).

Alley & Clarke (1992) also reported a large proportion of recycled Late Jurassic to Early Cretaceous palynomorphs within Upper Cretaceous (Turonian-Maastrichtian) sediments recovered from dredge sites in the eastern Ceduna and Duntroon sub-basins, though similar recycling is not observed in Turonian-Santonian mudstones recovered from IODP site U1512 in the western Ceduna sub-basin

(Wainman et al., 2020). Whilst Alley & Clarke (1992) ascribed a local source for the palynomorphs identified in dredge samples (particularly for Aptian-Albian dinoflagellates interpreted to have been reworked from eroded marine facies), it is possible that some of the palynomorphs were derived from Jurassic–Cretaceous sedimentary units that were deposited in the hinterland to these basins, but which now have been largely removed by erosion. This view is consistent with the AFTA data presented in this study, and from previous AFTA studies in the Adelaide Fold Belt (Gibson & Stüwe, 2000), Flinders Ranges (Tingate et al., 2007) and Officer Basin (Tingate & Duddy, 2002). These studies consistently show that exposed or subsurface rock samples mostly from the Lower Palaeozoic throughout this region were heated throughout the Mesozoic, prior to cooling beginning in the Late Cretaceous or early Cenozoic. This heating is interpreted to reflect the burial of these areas by a Mesozoic sedimentary sequence.

Independent support for this notion is provided by a provenance study of Santonian–Maastrichtian sediments recovered from the Gnarlyknots-1 well, which was drilled in the deepwater Ceduna sub-basin. MacDonald et al. (2013) presented U-Pb and fission track ages from 786 detrital zircon grains obtained from cuttings samples recovered by this well, and concluded that the dominant zircon populations were best explained by the recycling of Permian- to Early Cretaceous-age sedimentary sequences from the hinterland following Late Cretaceous exhumation.

We note that the concept of the accumulation of substantial thicknesses of Permian–Cretaceous sedimentary rocks over large areas of contemporary southern Australia stands at odds with some existing latest Palaeozoic-Mesozoic palaeogeographic reconstructions for Australia, which typically show the Fleurieu Peninsula and surrounding areas as emergent or undergoing erosion (Bradshaw &

Yeung, 1990; Brakel & Totterdell, 1996). This approach is common in many paleogeography studies, with areas of positive relief devoid of cover today interpreted as representing long term stable regions. A detailed reappraisal of the palaeogeography of this region is beyond the scope of this study, but should be a focus of future research guided by the growing body of data from low temperature thermochronology, in order to help better constrain the petroleum prospectivity of Mesozoic sedimentary basins located along the southern Australian margin (cf. Holford et al., 2010; MacDonald et al., 2012; Tassone et al., 2014, 2017). Improved tectonic models are also required incorporating this revised view, in order to explain the timing and style of continental breakup in eastern Gondwana, resulting in the formation of the conjugate southern Australian and Antarctic margins (e.g. Espurt et al., 2009; White et al., 2013).

*5.2.3. Cenozoic*

The preceding discussion has highlighted existing thermochronological and geochronological evidence for Cenozoic exhumation in a region surrounding the Fleurieu Peninsula. AFTA sample GC1069-33 from Port Elliot allows for the onset of cooling during the Late Cretaceous or later (beginning between 76 and 0 Ma), but results from Hallett Cove, Cape Jervis and Rosetta Head point to an early Cenozoic onset of exhumation, with cooling beginning after 56 Ma at Hallett Cove, after 50 Ma at Cape Jervis and after 47 Ma at Rosetta Head. Assuming that the late cooling episode recorded by AFTA represents the same event, sample GC545-2 from Sellicks Hill indicates that cooling and exhumation must have commenced prior to 26 Ma, whilst sample GC1069-66 from Hallett Cove indicates that cooling and exhumation must have commenced prior to 12 Ma.

We suggest that the cooling and exhumation most likely occurred during the early Cenozoic (Late Palaeocene–Early Eocene) (cf. Gibson & Stüwe, 2000) in conjunction with the development of the Cenozoic St Vincent Basin, which has been interpreted by some to be a flexural depression that developed in response to topographic loading following the compressional reactivation of the Mt Lofty and southern Flinders Ranges (Flöttmann & Cockshell, 1996). Preiss (2019) has suggested that compressional reactivation of the Willunga Fault commenced during the Eocene and is marked by a hiatus at the top of the North Maslin Sand during the Bartonian (McGowran et al., 2016). The evidence for the onlap of the Willunga Fault by Oligocene and Miocene strata indicates that the Willunga Scarp had been established by the mid-Cenozoic (Preiss, 2019). Given the presence of Late Oligocene to Middle Miocene age marine sediments in isolated intermontane basins such as the Myponga Basin and Hindmarsh Tiers Basin (Lindsay & Alley, 1995; Pledge et al., 2015), it is clear that Cenozoic exhumation and burial of the Fleurieu Peninsula was highly differential, and thus probably involved discrete fault reactivation (Preiss, 2019).

## 6. The preservation of ancient landscapes in the Australian continent: Implications for the tectonic stability of continental interiors

Our results are consistent with the findings of a series of recent studies into the preservation of pre-Cenozoic, Gondwana-era landforms across the Australian continent. The Western Australian Shield, including the Yilgarn and Pilbara cratons, is made up of Achaean and Proterozoic rocks, some of which date back to ~4 Ga (Wilde et al., 2001), and has generally been regarded as one of the most ancient landscapes on Earth (e.g. Jutson, 1914). Evidence for the subaerial exposure of the Yilgarn Craton during the Phanerozoic is provided by Permian–Carboniferous glacial deposits preserved along its eastern margin (Eyles and de Broekert, 2001) and by weathering imprints in open pit gold mines in the northern Yilgarn Craton that have been dated as Late Carboniferous and Late Cretaceous by palaeomagnetic data (Pillans, 2007). Apatite fission track data from the northern Yilgarn Craton presented by Weber et al. (2005) point to the pre-Permian exhumation of this region followed by re-burial of this region by ~3 km of Permian sediments, followed by exhumation leading to re-exposure by the Late Cretaceous (Pillans, 2007). Similarly, Belton et al. (2004) presented apatite fission track data supported by cosmogenic radionuclide ($^{10}Be$ and $^{26}Al$) analyses that bear on the evolution of the Ashburton Surface in the Tennant Creek area, a series of elevated (~500 m asl) planar ridge tops that have been purported by some authors to have been continuously exposed since the Cambrian (Stewart et al., 1986). However, Belton et al.'s (2004) results imply that this region was also buried beneath several kilometres of Palaeozoic–early Mesozoic sedimentary cover prior to exhumation that began during the latest Jurassic to Cretaceous. Similarly, in the Eastern Highlands in southeastern Australia, many ancient landscape remnants and associated regolith materials (e.g. deep weathering profiles) have been preserved alongside remnants of Mesozoic sedimentary cover (Hill, 1999). This is especially apparent on the margins of the Gippsland Basin at Wilsons Promontory and Phillip Island in Victoria (Hill, 1999).

The results of this study, when considered alongside those of Belton et al. (2004) and Weber et al. (2005), imply that much of the contemporary Australian continent experienced a strikingly coherent pattern of vertical motions from the late Phanerozoic onwards. Both the Fleurieu Peninsula, the northern Yilgarn Craton and the Pilbara Craton appear to express a record of Late Palaeozoic exhumation, perhaps representing distal responses to the intraplate Alice Springs Orogeny (e.g. Raimondo et al., 2014; Morón et al., 2020). Across the Fleurieu Peninsula and Yilgarn Craton this was followed by km-scale burial and the accumulation of a thick Permian-lower Mesozoic sedimentary cover. Renewed exhumation leading to the removal of much of this cover commenced variably during the Cretaceous–Cenozoic, possibly in response to the modification of stress regimes following the termination of subduction along eastern Gondwana and the evolving separation of southern Australia and Antarctica (Matthews et al., 2012; Holford et al., 2014). These observations lend support to the notion that repeated cycles of burial and exhumation are a characteristic feature of intraplate tectonic settings (Holford et al., 2009, 2010). Similar histories have been defined in other cratonic settings (e.g. Flowers and Kelley, 2011; Ault et al., 2013) as well as numerous passive margins (Green et al., 2013, 2018). Such cycles may be symptomatic of the responses of continental regions to oscillatory fluctuations of intraplate stress regimes (from extensional to compressional and vice versa) driven by changes in distant plate boundary activity over long (tens to hundreds of Myr) geological timescales (Sandiford, 2010). This oscillatory behaviour has played a central role in preserving ancient landscapes by burial prior to subsequent exhumation, not only in Australia but many other parts of the world (Green et al. 2013). Thus, the presence of ancient landscapes at the surface today is testimony to recent, rather than ancient, exposure.

**7. Conclusions**

Ancient geomorphic landforms that are preserved in the contemporary landscape provide an opportunity to assess the long-term tectonic stability of the continental crust. The occurrence of such features in parts of Australia has led some workers to argue for the long-term (i.e. hundreds of Myr) subaerial emergence of the

Australian landscape, but through the application of thermochronological tools such as apatite fission track analysis (AFTA), several recent studies have shown that some notable ancient (Early Palaeozoic) geomorphic features in Australia have experienced significant burial and exhumation during the Mesozoic and Cenozoic eras. In this study we applied AFTA to a suite of samples collected from localities in the Fleurieu Peninsula, southeastern Australia, that contain evidence for glacial erosion and thus subaerial exposure during the Early Permian. Our results suggest that the preserved rocks at these localities have been buried by ~1 km of now-eroded Permian–Mesozoic sedimentary cover prior to exhumation that probably began in the Paleogene. These findings have profound implications for palaeogeographic and tectonic reconstructions of this part of the Australian continent, whilst lending further credibility to the emerging view that burial and exhumation provides an effective mechanism for the preservation of ancient geomorphic features in the contemporary landscape.

**Acknowledgments**

This research was supported by ARC Discovery Project DP0879612. We thank various current and past members of the Stress, Structure and Seismic Research Group for field assistance, including Mark Tingay, Guillaume Backé, Rosalind King, Justin MacDonald and David Tassone. AFTA samples GC545-2, 3 and 4 were collected by the late Dave Gravestock. Elinor Alexander is acknowledged for helpful discussions regarding the Sellick Hill Formation. Finally, we are grateful to the Hotel Elliot for hosting many stimulating geological discussions.

**Figure Captions**

**Figure 1:** Late Carboniferous-Early Permian paleogeographic reconstruction of Gondwana, highlighting the extensive glaciations and sedimentary basins containing glacial or peri-glacial deposits. Modified after López-Gamundí (2010) and Blewett et al. (2012).

**Figure 2:** Simplified geological map of the Fleurieu Peninsula and surrounding regions, highlighting the main sampling localities and wells referred to in this study. Cross-section A-A' through the St Vincent, Myponga, Hindmarsh Tiers and Murray basins modified after Pledge et al. (2015). Seismic reflection profile B-B' showing the interpreted presence of a thick sequence Permian-Carboniferous offshore to the south of the Fleurieu Peninsula, modified after Flöttmann & Cockshell (1996).

**Figure 3:** (a) Photograph showing location of sample GC1069-33 at Knights Beach, Port Elliot. Sample was collected from the surface of a NE-striking joint plane, approximately 5 metres to the west of a glacially polished, striated surface developed on the Encounter Bay Granite (shown in inset). (b) Variation of fission track age with Chorine content for individual apatite grains within sample GC1069-33. (c) Plot of fission track length distribution for sample GC1069-33. (d) Thermal history solutions extracted from AFTA data from sample GC1069-33. As discussed in the text, our preferred interpretation is scenario 1.

**Figure 4:** (a) Photograph showing glacially polished, striated surface developed on siltstones of the Neoproterozoic Wilpena Group at Black Cliff, Hallett Cove. (b) Simplified geological map of Hallett Cove showing locations of samples GC1069-66 and 67, modified after Normington et al. (2018). (c) Variation of fission track age

with Chorine content for individual apatite grains within sample GC1069-66. (d) Plot of fission track length distribution for sample GC1069-66. (e) Thermal history solutions extracted from AFTA data from sample GC1069-66. (f) Variation of fission track age with Chorine content for individual apatite grains within sample GC1069-67. (g) Plot of fission track length distribution for sample GC1069-67. (h) Thermal history solutions extracted from AFTA data from sample GC1069-67.

**Figure 5:** (a) Simplified geological map of Cape Jervis showing locations of samples GC1069-68 and 69, modified after Normington et al. (2018). (b) Variation of fission track age with Chorine content for individual apatite grains within sample GC1069-68. (c) Plot of fission track length distribution for sample GC1069-68. (d) Thermal history solutions extracted from AFTA data from sample GC1069-68. (e) Variation of fission track age with Chorine content for individual apatite grains within sample GC1069-69. (f) Plot of fission track length distribution for sample GC1069-69. (g) Thermal history solutions extracted from AFTA data from sample GC1069-69.

**Figure 6:** (a) Photograph showing glacially polished, striated surface developed on Kanmantoo Group metasedimentary rocks at Inman Valley, and location of AFTA sample GC1069-70. (b) Variation of fission track age with Chorine content for individual apatite grains within sample GC1069-70. (c) Plot of fission track length distribution for sample GC1069-70. (d) Thermal history solutions extracted from AFTA data from sample GC1069-70.

**Figure 7:** (a) Variation of fission track age with Chorine content for individual apatite grains within sample GC1069-71. (b) Plot of fission track length distribution for

sample GC1069-71. (c) Thermal history solutions extracted from AFTA data from sample GC1069-71.

**Figure 8:** (a) Variation of fission track age with Chorine content for individual apatite grains within sample GC545-2. (b) Plot of fission track length distribution for sample GC545-2. (c) Thermal history solutions extracted from AFTA data from sample GC545-2.

**Figure 9:** (a) Variation of fission track age with Chorine content for individual apatite grains within sample GC545-3. (b) Plot of fission track length distribution for sample GC545-3. (c) Thermal history solutions extracted from AFTA data from sample GC545-3. (d) Variation of fission track age with Chorine content for individual apatite grains within sample GC545-4. (e) Plot of fission track length distribution for sample GC545-4. (f) Thermal history solutions extracted from AFTA data from sample GC545-4.

**Figure 10:** Comparison of the timing information derived from all AFTA data that show evidence for higher palaeotemperatures post-deposition or intrusion. Synthesis of results identifies a number of discrete phases of cooling, indicated by the vertical bands. Grey boxes indicate the range of stratigraphic ages for single samples. Horizontal bands define range of timing for the onset of cooling derived from AFTA data in each sample within a 95% confidence interval. The timing constraints from AFTA data are compared with AFTA results from the Otway Basin, the generalized stratigraphy of the study area and the proximal Ceduna sub-basin, and with co-eval

plate tectonic events (after Holford et al., 2011a; MacDonald et al., 2013; Raimondo et al., 2014).

**Figure 11:** Simplified geological map of the Fleurieu Peninsula emphasising the observed and inferred locations of faults that exhibit evidence for displacement during the Cenozoic, in relation to the surface distribution of Cenozoic and Permian-Carboniferous sedimentary rocks. The map also highlights AFTA samples that exhibit evidence for cooling at some point during the Cenozoic, with associated constraints on the temperature and timing of the cooling in individual samples.

**Figure 12:** Diagram showing constraints on estimated present-day temperatures as a function of depth in the Stansbury West-1 well in the Yorke Peninsula. Note the elevated geothermal gradient associated with the Permian strata, implying that these rocks have lower thermal conductivity than the underlying Cambrian sequence.

**References**

Alexander, E.M., Gravestock, D.I., 1990. Sedimentary facies in the Sellick Hill Formation, Fleurieu Peninsula, South Australia. Geological Society of Australia Special Publication 16, 269-225.

Alley, N.F., Bourman, R.P., 1984. Sedimentology and origin of late Palaeozoic glacigene deposits at Cape Jervis, South Australia. Royal Society of South Australia Transactions 108, 63-75.

Alley, N.F., Clarke, J.D.A., 1992. Stratigraphy and palynology of Mesozoic sediments from the Great Australian Bight area, southern Australia. BMR Journal of Australian Geology and Geophysics 13, 113-129.

Alley, N.F., Bourman, R.P., Gravestock, D.I., Hibburt, J.E., Hill, A.J., Rankin, L.R., 1995. Late Palaeozoic. In: Drexel, J.F., Preiss, W.V. (Eds.) The Geology of South Australia, Volume 2, The Phanerozoic. South Australia, Geological Survey, Bulletin 54, pp 63–91.

Alley, N.F., Bourman, R.P., Milnes, A.R. 2013. Late Palaeozoic Troubridge Basin sediments on Kangaroo Island, South Australia. MESA Journal 70, 24–43.

Ault, A.K., Flowers, R.M., Bowring, S.A., 2013. Phanerozoic surface history of the Slave craton. Tectonics 32, 1066-1083.

Belton, D.X., Brown, R.W., Kohn, B.P., Fink, D., Farley, K.A., 2004. Quantitative resolution of the debate over antiquity of the central Australian landscape: implications for the tectonic and geomorphic stability of cratonic interiors. Earth and Planetary Science Letters 219, 21-34.

Blewett, R.S., Kennett, B.L.M., Huston, D.L., 2012. Australian in time and space. In: Shaping a Nation: A Geology of Australia, Blewett R.S. (Ed.), Geoscience Australia and ANU E Press, Canberra, 47–119.

Boone, S.C., Seiler, C., Reid, A.J., Kohn, B., Gleadow, A., 2016. An Upper Cretaceous paleo-aquifer system in the Eromanga Basin of the central Gawler Craton, South Australia: evidence from apatite fission track thermochronology. Australian Journal of Earth Sciences 63, 315-331.

Bourman, R.P., Lindsay, J.M., 1989. Timing, extent and character of late Cainzoic faulting on the eastern margin of the Mt Lofty Ranges, South Australia. Transactions of the Royal Society of South Australia 113, 63-67.

Bourman, R.P., Alley, N.F., 1990. Stratigraphy and environments of deposition at Hallett Cove during the Late Palaeozoic. Mines and Energy Review South Australia 157, 68–82.

Bradshaw, M., Yeung, M., 1990. The Jurassic palaeogeography of Australia. Bureau of Mineral Resources, Australia, Record 1990/76, 1–60.

Brakel, A.T., Totterdell, J.M., 1996. Palaeogeographic atlas of Australia, Vol. 6, Permian, Australian Geological Survey Organization, Canberra, pp. 1–38.

Clark, D., McPherson, A., Van Dissen, R., 2012. Long-term behaviour of Australian stable continental region (SCR) faults. Tectonophysics 566, 1-30.

Crowell, J.C, Frakes, L.A., 1971. Late Palaeozoic glaciation of Australia. Australian Journal of Earth Sciences 17, 115–155.

Czarnota, K., Roberts, G.G., White, N.J., Fishwick, S., 2014. Spatial and temporal patterns of Australian dynamic topography from River Profile Modeling. Journal of Geophysical Research: Solid Earth 119, 1384-1424.

Daily, B., Twidale, C.R., Milnes, A.R., 1974. The age of the lateritized summit surface on Kangaroo Island and adjacent regions of South Australia. Journal of the Geological Society of Australia 21, 387-392.

Dasch, E.J., Milnes, A.R., Nesbitt, R.W., 1971. Rubidium-strontium geochronology of the Encounter Bay Granite and adjacent metasedimentary rocks, South Australia. Journal of the Geological Society of Australia 18, 259-266.

Davies, J.L., Williams, M.A., 1978. Landform evolution in Australasia. Australian National University Press.

Duddy, I.R., 2003. Mesozoic: a time of change in tectonic regime. In: Birch, W.D. (Ed.) Geology of Victoria, Geological Society of Australia Victoria Division Vol. 23, pp. 239-286.

Eyles, S.N, de Broekert, P., 2001. Glacial tunnel valleys in the Eastern Goldfields of Western Australia cut below the Late Palaeozoic Pilbara ice sheet. Palaeogeography, Palaeoclimatology, Palaeoecology 171, 29–40

Espurt, N., Callot, J.P., Totterdell, J., Struckmeyer, H., Vially, R., 2009. Interactions between continental breakup dynamics and large-scale delta system evolution: Insights from the Cretaceous Ceduna delta system, Bight Basin, Southern Australian margin. Tectonics 28, TC6002,

Fielding, C.R., Frank, T.D., Birgenheier, L.P., Rygel, M.C., Jones, A.T., Roberts, J., 2008. Stratigraphic imprint of the Late Palaeozoic Ice Age in eastern Australia: a record of alternating glacial and nonglacial climate regime. Journal of the Geological Society 165, 129-140.

Flöttmann, T., Cockshell, C.D., 1996. Palaeozoic basins of southern South Australia: New insights into their structural history from regional seismic data. Australian Journal of Earth Sciences 43, 45-55.

Flowers, R.M., Kelley, S.A., 2011. Interpreting data dispersion and "inverted" dates in apatite (U-Th)/He and fission-track datasets: An example from the US midcontinent. Geochimica et Cosmochimica Acta 75, 5169-5186.

Foden, J., Elburg, M.A., Dougherty-Page, J., Burtt, A., 2006. The timing and duration of the Delamerian Orogeny: correlation with the Ross Orogen and implications for Gondwana assembly. The Journal of Geology 114, 189-210.

Gale, S.J., 1992. Long-term landscape evolution in Australia. Earth Surface Processes and Landforms 17, 323-343.

Gibson, H.J., Stüwe, K., 2000. Multiphase cooling and exhumation of the southern

Adelaide Fold Belt: constraints from apatite fission track data. Basin Research 12, 31-45.

Gibson, H.J, Duddy, I.R., Ambrose, G.J., Marshall, T.R, 2005. Regional perspectives on new and reviewed thermal history data from central Australian basins. In Northern Territory Geological Survey (editors). Symposium handbook. Central Australian Basins Symposium: Petroleum and minerals potential. Alice Springs, 16–18 August 2005, 22.

Gleadow, A.J.W., Duddy, I.R., 1981. A natural long-term track annealing experiment for apatite. Nuclear Tracks 5, 169-174.

Gleadow, A.J., Kohn, B.P., Brown, R.W., O'Sullivan, P.B., Raza, A., 2002. Fission track thermotectonic imaging of the Australian continent. Tectonophysics 349, 5-21.

Gravestock, D.I., 1995. Early and Middle Palaeozoic. In: Drexel, J.F., Preiss, W.V. (Eds.) The Geology of South Australia, Volume 2, The Phanerozoic. South Australia, Geological Survey, Bulletin 54, pp 3–61.

Green, P.F., Duddy, I., 2012. Thermal history reconstruction in sedimentary basins using apatite fission-track analysis and related techniques. In: Analyzing the Thermal History of Sedimentary Basins: Methods and Case Studies: SEPM Special Publication 103. pp. 65–104.

Green, P.F, Duddy, I.R. 2020. Discussion: Extracting thermal history from low temperature thermochronology. A comment on recent exchanges between Vermeesch and Tian and Gallagher and Ketcham. Earth-Science Reviews, 103197.

Green, P.F., Duddy, I.R. and Hegarty, K.A., 2002. Quantifying exhumation from apatite fission-track analysis and vitrinite reflectance data: precision, accuracy and latest results from the Atlantic margin of NW Europe. Geological Society, London, Special Publications 196, 331-354.

Green, P.F., Lidmar-Bergström, K., Japsen, P., Bonow, J.M., Chalmers, J.A., 2013. Stratigraphic landscape analysis, thermochronology and the episodic development of elevated passive continental margins. Geological Survey of Denmark and Greenland Bulletin 2013/30, 150 pp.

Green, P.F., Japsen, P., Chalmers, J.A., Bonow, J.M. & Duddy, I.R. 2018: Post-breakup burial and exhumation of passive continental margins: Seven propositions to inform geodynamic models. Gondwana Research **53**, 58–81

Haines, P.W., Jago, J.B., Gum, J.C., 2001. Turbidite deposition in the Cambrian Kanmantoo Group, South Australia. Australian Journal of Earth Sciences 48, 465-478.

Hall, J.W., Glorie, S., Collins, A.S., Reid, A., Evans, N., McInnes, B., Foden, J., 2016. Exhumation history of the Peake and Denison Inliers: insights from low-temperature thermochronology. Australian Journal of Earth Sciences 63, 805-820.

Hill, S.M., 1999. Mesozoic regolith and palaeolandscape features in southeastern Australia: significance for interpretations of denudation and highland evolution. Australian Journal of Earth Sciences 46, 217-232.

Hillis, R.R., Holford, S.P., Green, P.F., Doré, A.G., Gatliff, R.W., Stoker, M.S., Thomson, K., Turner, J.P., Underhill, J.R., Williams, G.A., 2008. Cenozoic exhumation of the southern British Isles. Geology 36, 371-374.

Holford, S.P., Green, P.F., Duddy, I.R., Turner, J.P., Hillis, R.R., Stoker, M.S., 2009. Regional intraplate exhumation episodes related to plate-boundary deformation. Geological Society of America Bulletin 121, 1611-1628.

Holford, S., Hillis, R., Duddy, I., Green, P., Tuitt, A., Stoker, M., 2010. Impacts of Neogene-Recent compressional deformation and uplift on hydrocarbon prospectivity of the passive southern Australian margin. The APPEA Journal 50, 267-286.

Holford, S.P., Hillis, R.R., Hand, M., Sandiford, M., 2011a. Thermal weakening localizes intraplate deformation along the southern Australian continental margin. Earth and Planetary Science Letters 305, 207-214.

Holford, S., Hillis, R., Duddy, I., Green, P., Stoker, M., Tuitt, A., Backé, G., Tassone, D., MacDonald, J., 2011b. Cenozoic post-breakup compressional deformation and exhumation of the southern Australian margin. The APPEA Journal 51, 613-638.

Holford, S.P., Tuitt, A.K., Hillis, R.R., Green, P.F., Stoker, M.S., Duddy, I.R., Sandiford, M., Tassone, D.R., 2014. Cenozoic deformation in the Otway Basin, southern Australian margin: implications for the origin and nature of post-breakup compression at rifted margins. Basin Research 26, 10-37.

Howchin, W., 1924. The Recent extinction of certain marine animals of the southern coast of Australia, together with other facts that are suggestive of a change in climate. Australasian Association for the Advancement of Science Report 16, 94-101.

Jenkins, R.J., Sandiford, M., 1992. Observations on the tectonic evolution of the southern Adelaide Fold Belt. Tectonophysics 214, 27-36.

Jennings, J.N, Mabbutt, J.A., 1967. Landform Studies from Australia and New Guinea. Cambridge University Press, New York, 434 pp.

Jutson, J.T. 1914., Physiographical geology (physiography) of Western Australia. Geological Survey of Western Australia Bulletin 61, Government Printer, Perth.

King, L.C., 1950. The cyclic land-surfaces of Australia. Journal of the Royal Society of Victoria 62. 79–95.

Kohn, B.P., Gleadow, A.J.W., Brown, R.W., Gallagher, K., O'Sullivan, P.B., Foster, D.A., 2002. Shaping the Australian crust over the last 300 million years: insights from fission track thermotectonic imaging and denudation studies of key terranes. Australian Journal of Earth Sciences 49, 697-717.

Lidmar-Bergström, K. Bonow, J.M., Japsen, P., 2013. Stratigraphic Landscape Analysis and geomorphological paradigms: Scandinavia as an example of Phanerozoic uplift and subsidence. Global and Planetary Change 100, 153–171.

Lindsay, J.M., Alley, N.F., 1995. Myponga and Hindmarsh Tiers Basins. In: Drexel, J.F., Preiss, W.V. (Eds.) The Geology of South Australia, Volume 2, The Phanerozoic. South Australia, Geological Survey, Bulletin 54, pp 199-201.

López-Gamundí, O.R, 2010. Late Paleozoic glacial events and postglacial transgressions in Gondwana, Geological Society of America Special Papers 468.

Lubiniecki, D.C., White, S.R., King, R.C., Holford, S.P., Bunch, M.A., Hill, S.M., 2019. Structural evolution of carbonate-hosted cataclastic bands adjacent to a major neotectonic fault, Sellicks Beach, South Australia. Journal of Structural Geology 126, pp.11-24.

Lubiniecki, D.C., King, R.C., Holford, S.P., Bunch, M.A., Hore, S.B., Hill, S.M., 2020. Cenozoic structural evolution of the Mount Lofty Ranges and Flinders Ranges, South Australia, constrained by analysis of deformation bands. Australian Journal of Earth Sciences, pp.1-19.

MacDonald, J., Backé, G., King, R., Holford, S., Hillis, R., 2012. Geomechanical modelling of fault reactivation in the Ceduna Sub-basin, Bight Basin, Australia. Geological Society, London, Special Publications 367, 71-89.

MacDonald, J.D., Holford, S.P., Green, P.F., Duddy, I.R., King, R.C., Backé, G., 2013. Detrital zircon data reveal the origin of Australia's largest delta system. Journal of the Geological Society 170, 3-6.

Matthews, K.J., Seton, M., Müller, R.D., 2012. A global-scale plate reorganization event at 105– 100 Ma. Earth and Planetary Science Letters 355, 283-298.

Metcalfe, I., Crowley, J.L., Nicoll, R.S., Schmitz, M., 2015. High-precision U-Pb CA-TIMS calibration of Middle Permian to Lower Triassic sequences, mass extinction and extreme climate-change in eastern Australian Gondwana. Gondwana Research 28, 61-81.

Milnes, A., Bourman, R., 1972. A Late Palaeozoic glaciated granite surface at Port Elliot, South Australia. Royal Society of South Australia Transactions 96, 149-155.

Milnes, A.R., Compston, W., Daily, B., 1977. Pre-to syn-tectonic emplacement of early Palaeozoic granites in southeastern South Australia. Journal of the Geological Society of Australia 24, 87-106.

Mitchell, M.M., Kohn, B.P., O'Sullivan, P.B., Hartley, M.J., Foster, D.A., 2002. Low-temperature thermochronology of the Mt Painter Province, South Australia. Australian Journal of Earth Sciences 49, 551-563.

Morón, S., Kohn, B.P., Beucher, R., Mackintosh, V., Cawood, P.A., Moresi, L., Gallagher, S.J., 2020. Denuding a craton: Thermochronology record of Phanerozoic unroofing from the Pilbara Craton, Australia. Tectonics 39, e2019TC005988.

Normington, V., Hill, S.M., Tiddy, C.J. and Giles, D., 2018. Sedimentology of the late Palaeozoic Cape Jervis Formation, Troubridge Basin, South Australia. Department for Energy and Mining.

Nott, J., 1995. The antiquity of landscapes on the north Australian craton and the implications for theories of long-term landscape evolution. The Journal of Geology 103, 19-32.

Pillans, B., 2005. Geochronology of the Australian regolith. Regolith Landscape Evolution Across Australia. CRC LEME, 41-52.

Pillans, B., 2007. Pre-Quaternary landscape inheritance in Australia. Journal of

Quaternary Science 22, 439-447.

Pledge, N., Milnes, A., Bourman, R. and Alley, N., 2015. Fossil shark teeth from upland Fleurieu Peninsula, South Australia: evidence for previously unknown Tertiary marine sediments. MESA Journal 76, 67-73.

Preiss, W.V., 2019. The tectonic history of Adelaide's scarp-forming faults. Australian Journal of Earth Sciences 66, 305-365.

Quigley, M.C., Clark, D. and Sandiford, M., 2010. Tectonic geomorphology of Australia. Geological Society, London, Special Publications 346, 243-265.

Raimondo, T., Hand, M., Collins, W.J., 2014. Compressional intracontinental orogens: Ancient and modern perspectives. Earth-Science Reviews 130, 128-153.

Sandiford, M., 2003. Neotectonics of southeastern Australia: linking the Quaternary faulting record with seismicity and in situ stress. Geological Society of America Special Paper 372, 107-119.

Sandiford, M., 2010. Why are the continents just so…?. Journal of Metamorphic Geology, *28*(6), pp.569-577.

Selwyn, A.R., 1860. Geological notes of a journey in South Australia from Cape Jervis to Mount Serle. Proceedings of the Royal Geographical Society of London, 242-244.

Shaw, R.D., Etheridge, M.A., Lambeck, K., 1991. Development of the Late Proterozoic to Mid-Paleozoic, intracratonic Amadeus Basin in central Australia: A key to understanding tectonic forces in plate interiors. Tectonics 10, 688-721.

Stewart, A.J., Blake, D.H., Ollier, C.D., 1986. Cambrian river terraces and ridgetops in central Australia: oldest persisting landforms?. Science 233, 758-761.

Tassone, D.R., Holford, S.P., Duddy, I.R., Green, P.F., Hillis, R.R., 2014. Quantifying Cretaceous–Cenozoic exhumation in the Otway Basin, southeastern Australia, using sonic transit time data: Implications for conventional and unconventional hydrocarbon prospectivity. AAPG Bulletin 98, 67-117.

Tassone, D.R., Holford, S.P., King, R., Tingay, M.R., Hillis, R.R., 2017. Contemporary stress and neotectonics in the Otway Basin, southeastern Australia. Geological Society, London, Special Publications 458, 49-88.

Tate, R., 1879. Leading physical features of South Australia. Royal Society of South Australia Transactions 2, 64.

Tingate, P.R., Duddy, I.R., 2002. The thermal history of the eastern Officer Basin (South Australia): evidence from apatite fission track analysis and organic maturity data. Tectonophysics 349, 251-275.

Tingate, P.R., Green, P.F., Lemon, N.M., McKirdy, D.M., 2007. Insights into the tectonic development and hydrocarbon potential of the Flinders Ranges, South Australia, based on AFTA® and organic maturity data from the Blinman-2 borehole. Central Australian Basins Symposium 2, 1-12.

Tokarev, V., Sandiford, M., Gostin, V., 1999. Landscape evolution in the Mount Lofty Ranges: implications for regolith development. In New approaches to an old continent, 3rd Australian Regolith Conference Proceedings, Regolith 98, 127-134.

Turner, S., Haines, P., Foster, D., Powell, R., Sandiford, M., Offler, R., 2009. Did the Delamerian Orogeny start in the Neoproterozoic?. The Journal of Geology 117, 575-583.

Twidale, C.R., 1998. Antiquity of landforms: an 'extremely unlikely' concept vindicated. Australian Journal of Earth Sciences 45, 657-668.

Wainman, C.C., Tagliaro, G., Jones, M.M., Charles, A.J., Hall, T., White, L.T., Bogus, K.A., Wolfgring, E., O'Connor, L.K., McCabe, P.J., Holford, S.P., 2020. The sedimentological evolution and petroleum potential of a very thick Upper Cretaceous marine mudstone succession from the southern high latitudes—a case study from the Bight Basin, Australia. Marine and Petroleum Geology, 104441.

Weber, U.D., Kohn, B.P., Gleadow, A.J.W., Nelson, D.R., 2005. Low temperature Phanerozoic history of the Northern Yilgarn Craton, Western Australia. Tectonophysics 400, 127-151.

White, L.T., Gibson, G.M., Lister, G.S., 2013. A reassessment of paleogeographic reconstructions of eastern Gondwana: Bringing geology back into the equation. Gondwana Research 24, 984-998.

Wilde, S.A., Valley, J.W., Peck, W.H., Graham, C.M., 2001. Evidence from detrital zircons for the existence of continental crust and oceans on the Earth 4.4 Gyr ago. Nature 409, 175-178.

Wopfner, H., 1972. Climate and deposition in Permian and Early Triassic in South Australia. Abstracts 44th ANZAAS Congress Sydney, 95-96.

# Holford et al Figure 1

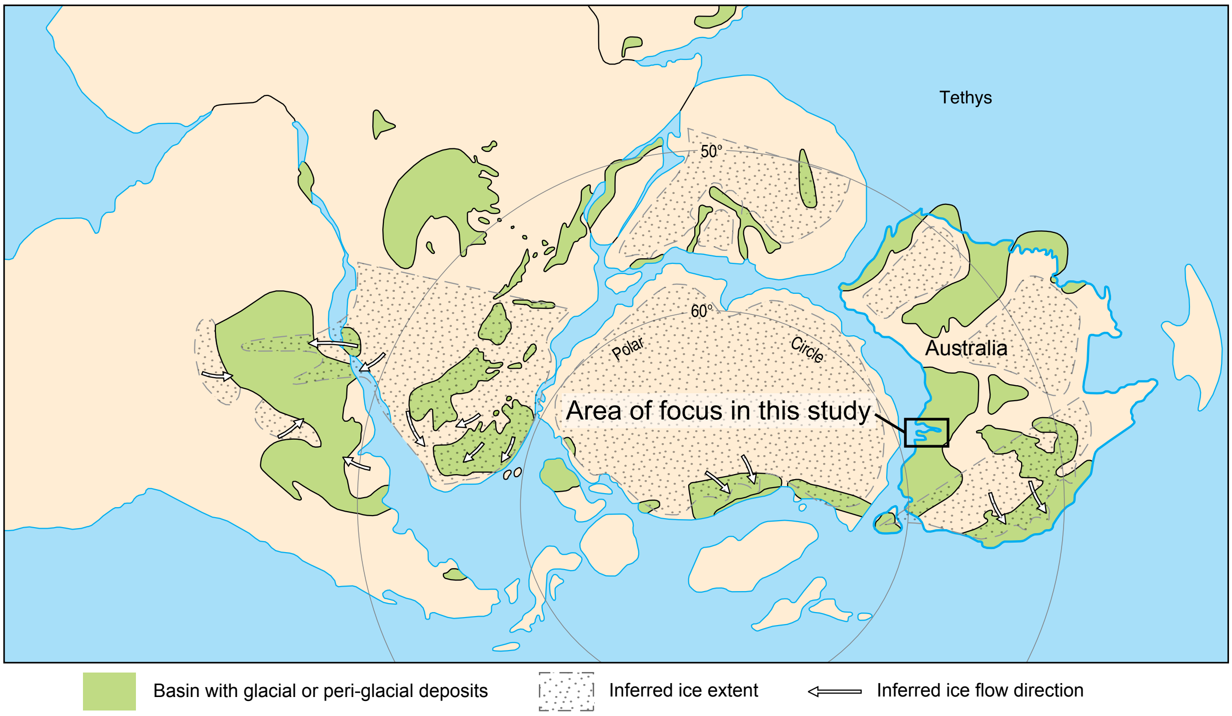

**Holford et al Figure 2**

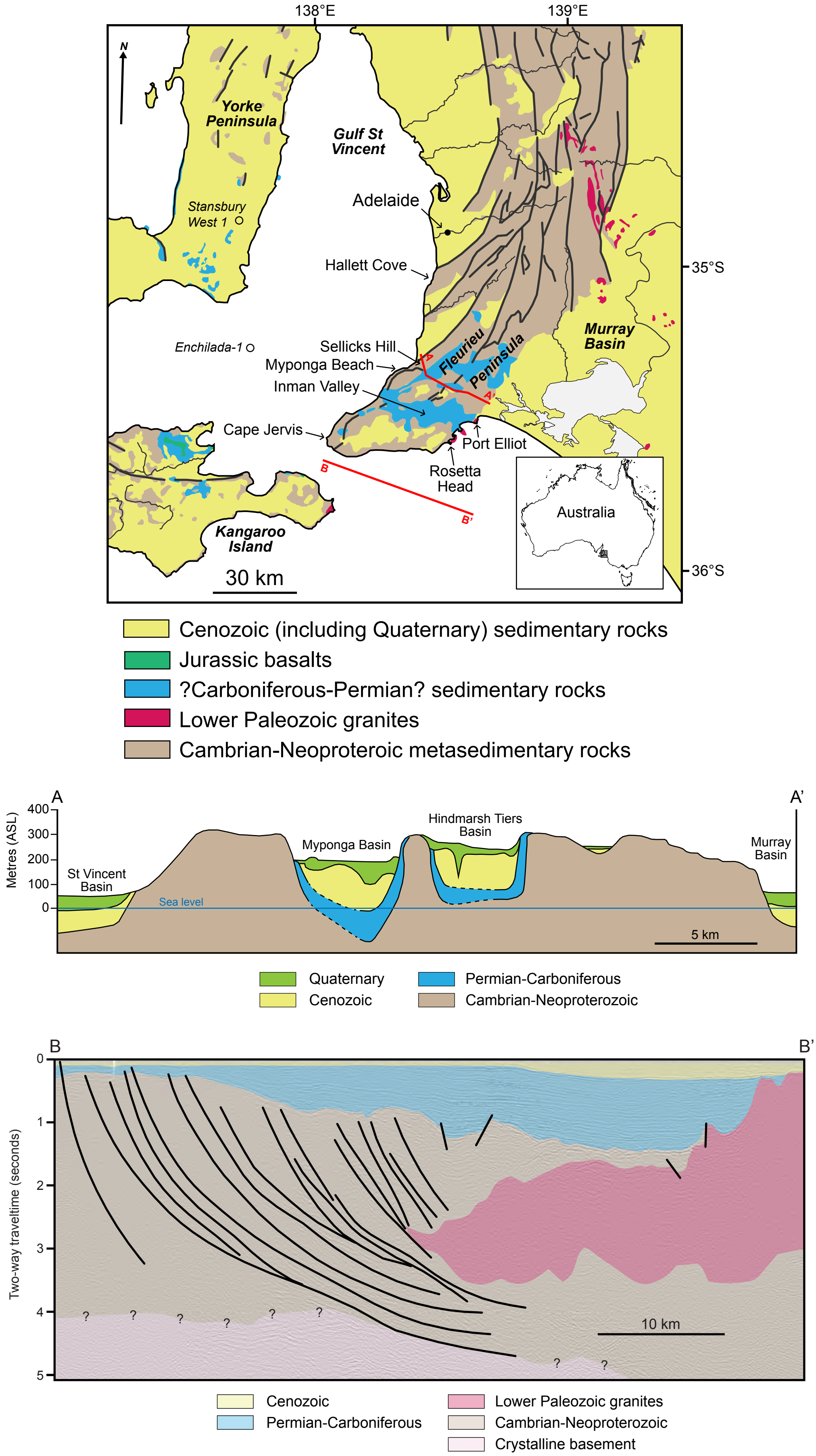

**Holford et al Figure 3**

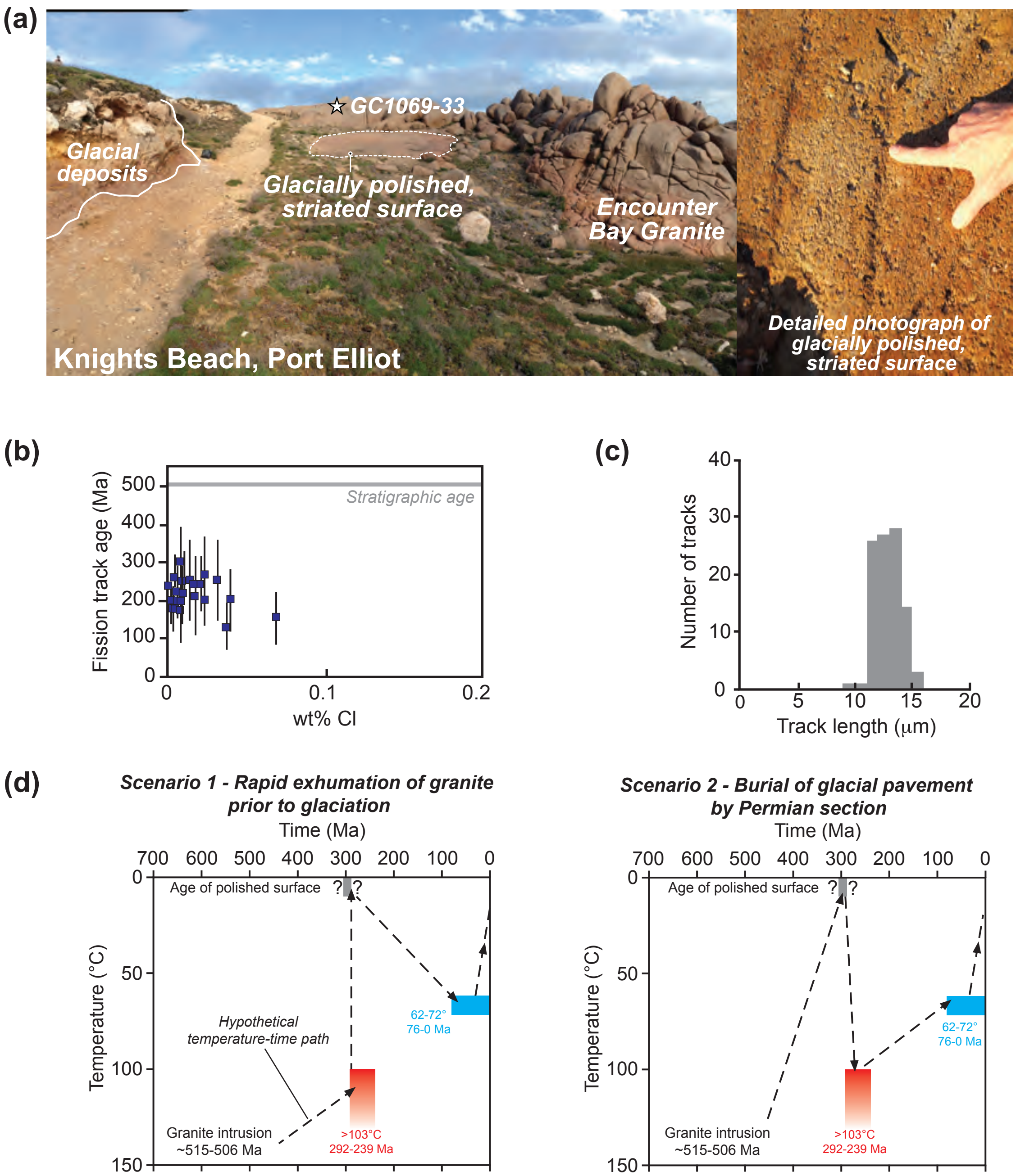

Holford et al Figure 4

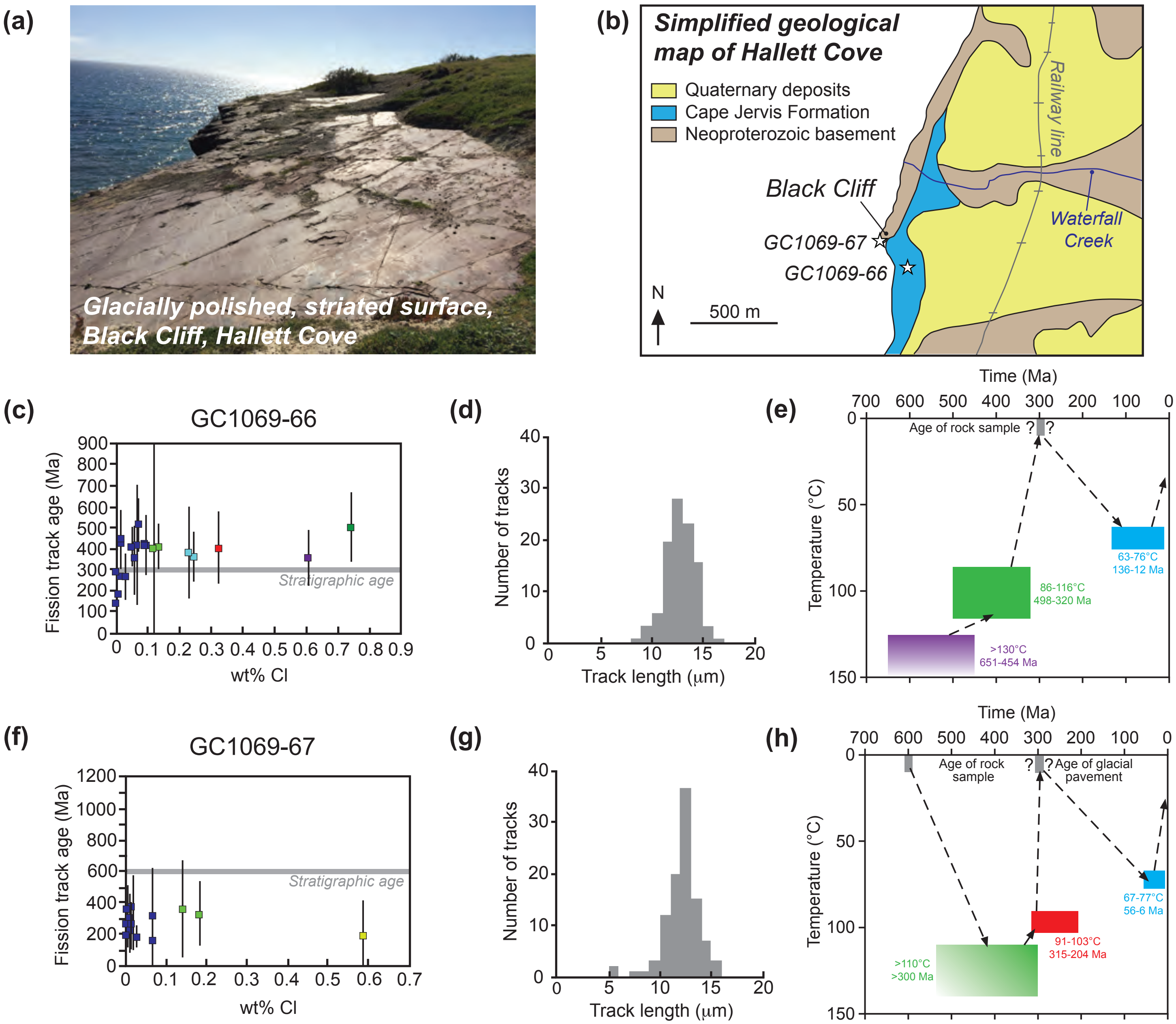

**Holford et al Figure 5**

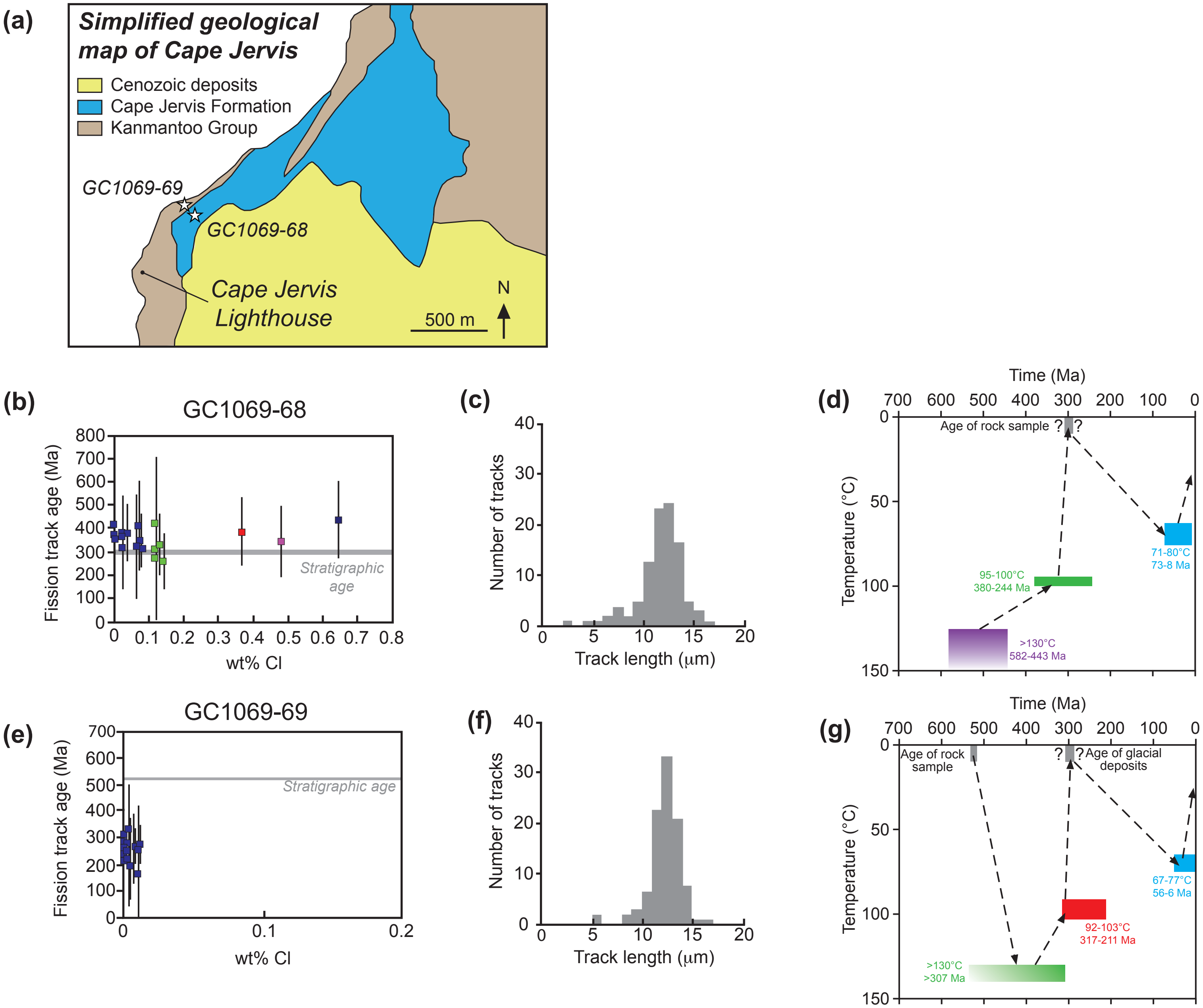

**Holford et al Figure 6**

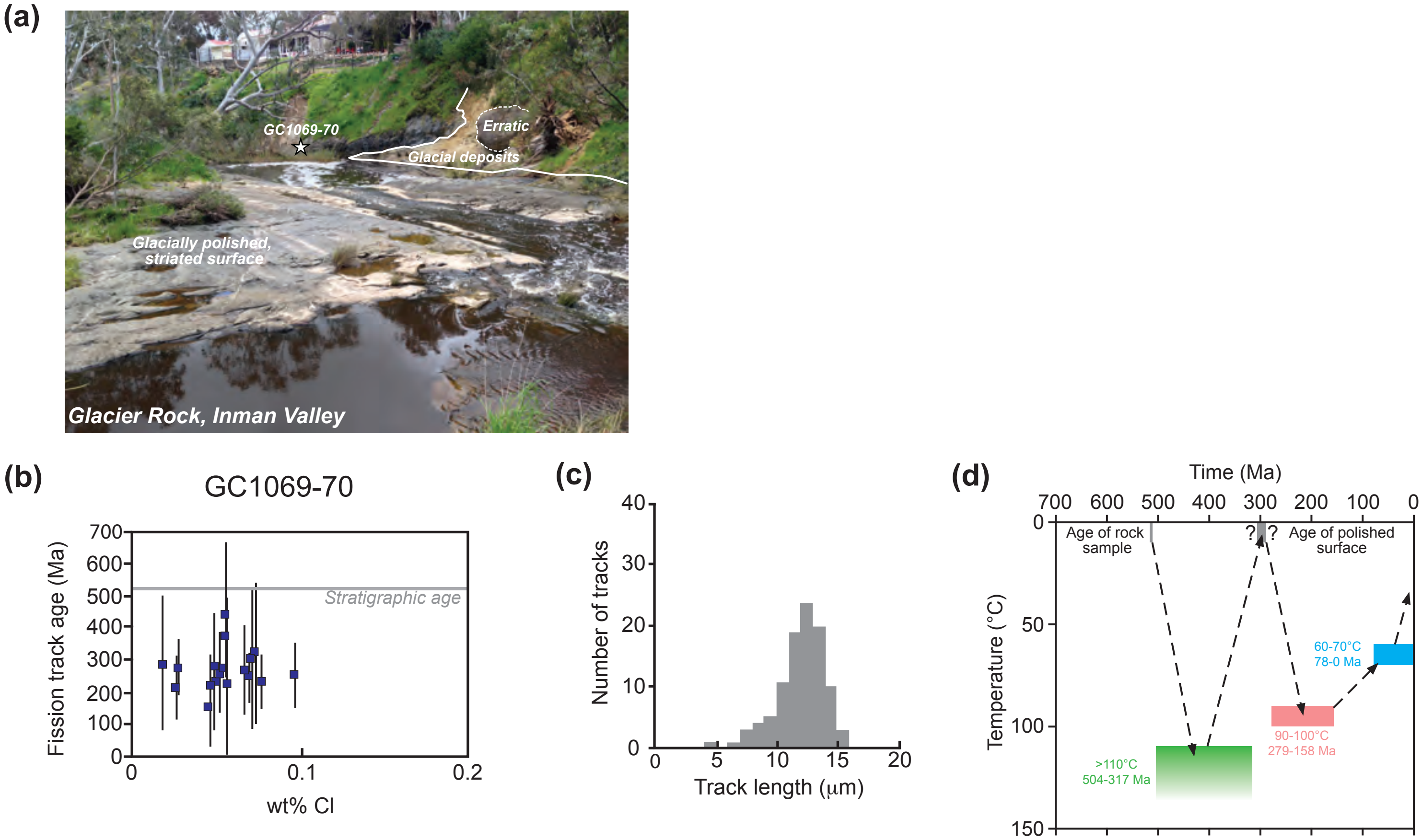

**Holford et al Figure 7**

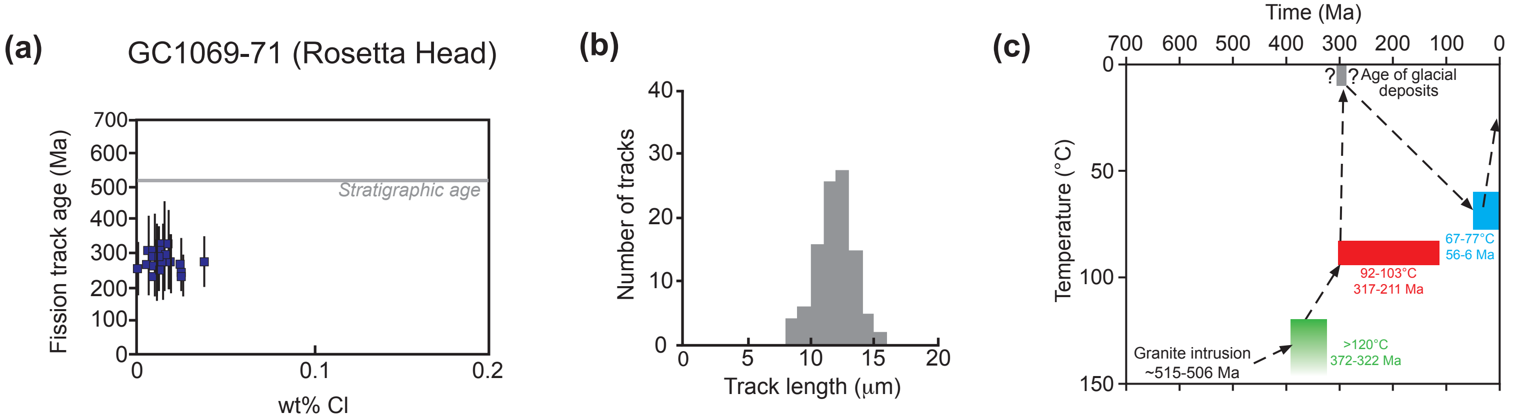

**Holford et al Figure 8**

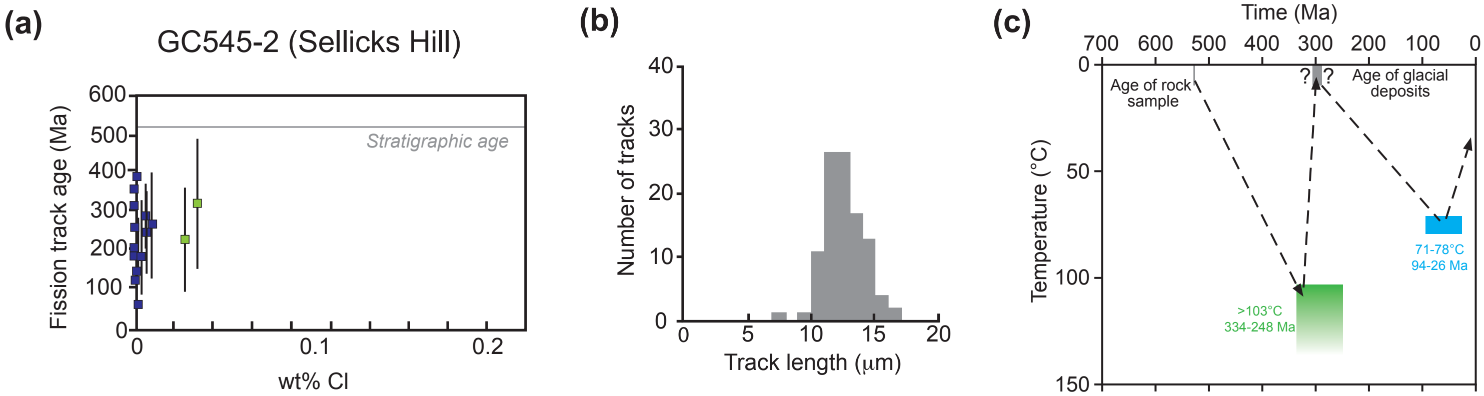

## Holford et al Figure 9

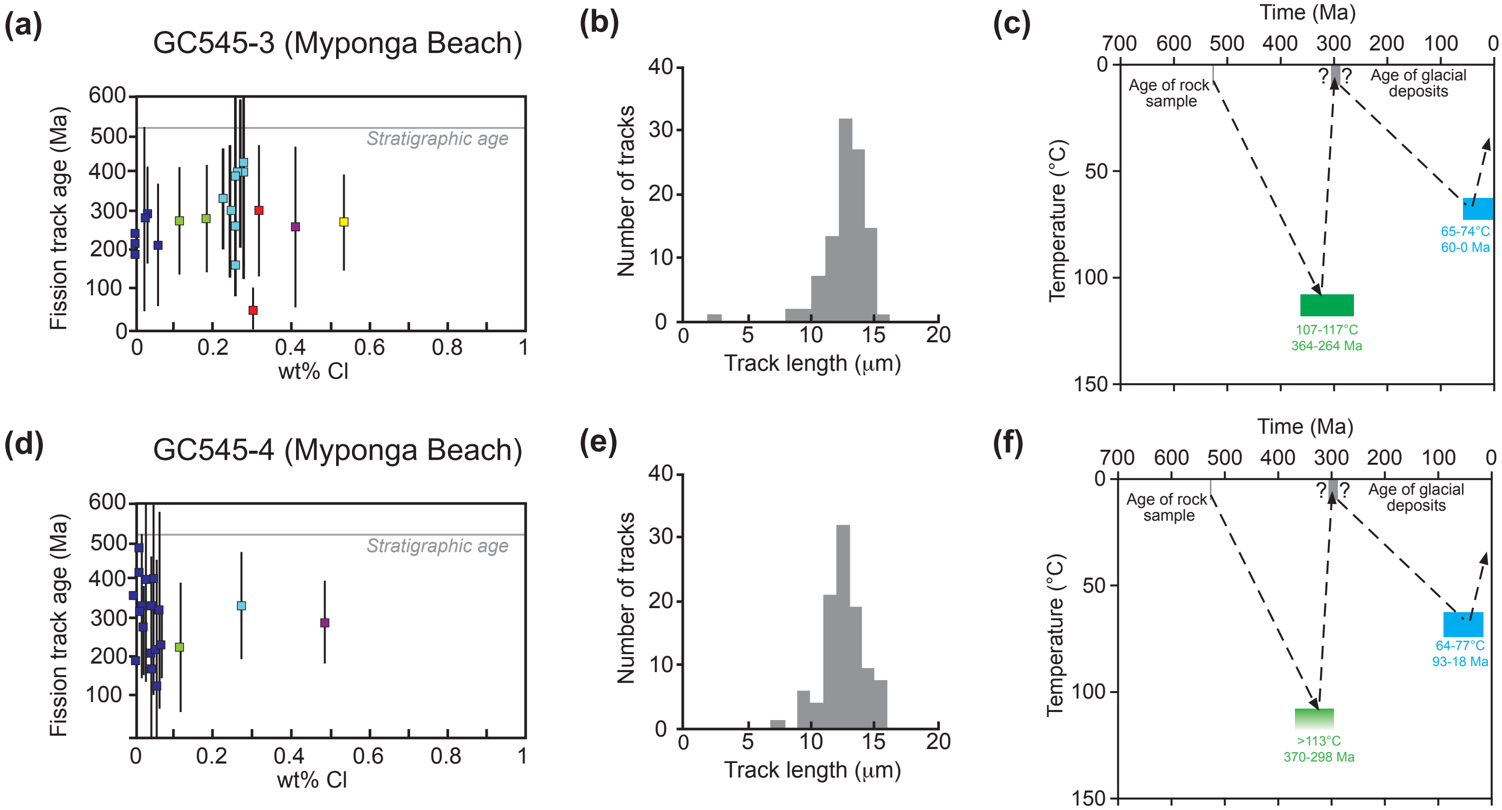

# Holford et al Figure 10

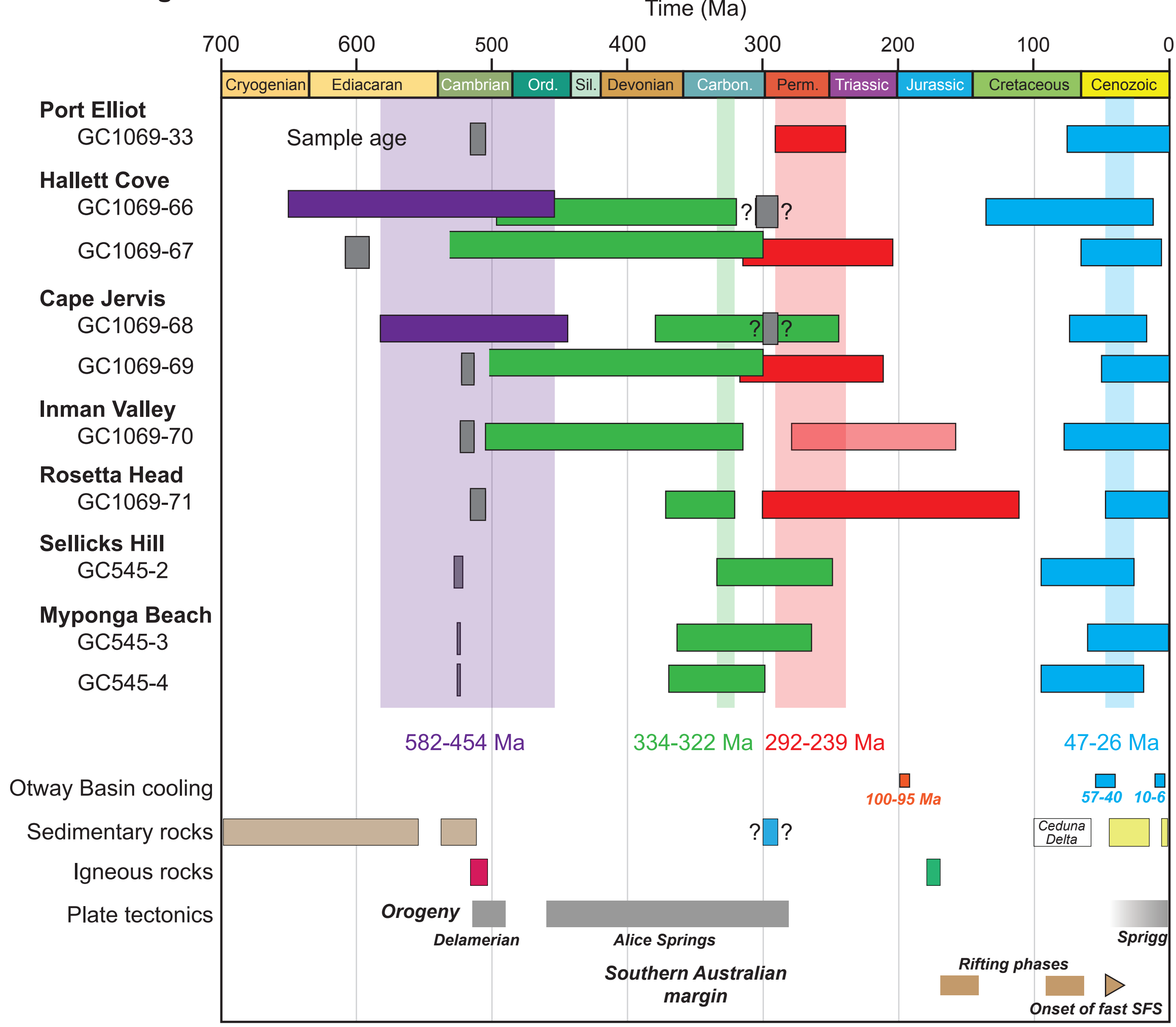

Holford et al Figure 11

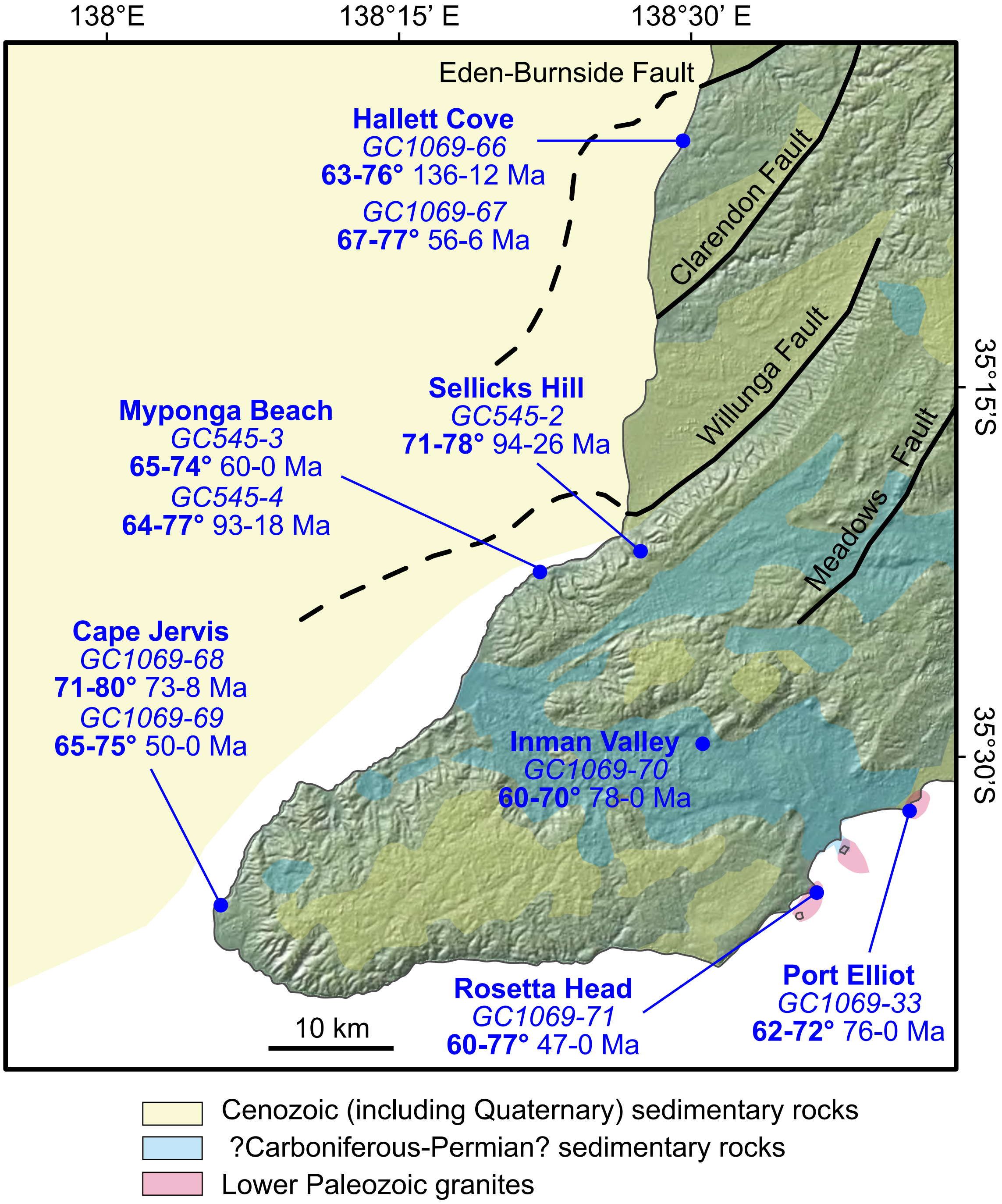

**Holford et al Figure 12**

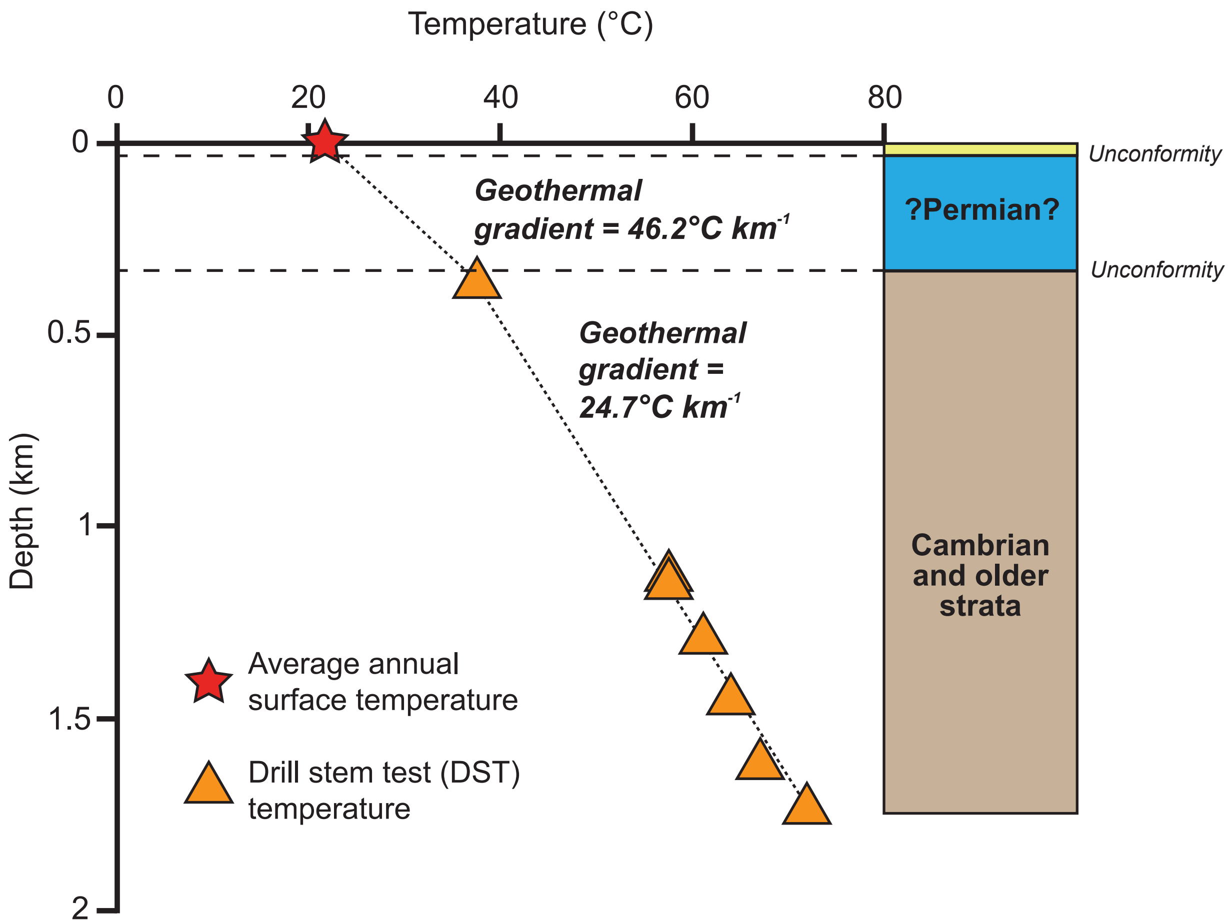

| Sample number | Sample location | Latitude/ longitude | Stratigraphic unit/division | Stratigraphic age (Ma) | $\rho_D$‡ ($10^6$ tracks $cm^{-2}$) | $\rho_s$‡ ($10^6$ tracks $cm^{-2}$) | $\rho_i$‡ ($10^6$ tracks $cm^{-2}$) | $P(\chi^2)$ § (%) (no. of grains) | Fission track age¶ (Ma) | Mean track length ¦ (µm) | Std dev* (µm) | Thermal history constraints†† |
|---|---|---|---|---|---|---|---|---|---|---|---|---|
| GC1069-33 | Port Elliot | -35.536476, 138.679234 | Encounter Bay Granite, Upper Cambrian | 515-506 | 1.387 (2,230) | 3.526 (1,398) | 4.038 (1,601) | 26 (20) | 226.3±10.2 | 12.85±0.11 (104) | 1.12 | >103°C, 292-239 Ma<br>62-72°C, 76-0 Ma |
| GC1069-66 | Hallett Cove | -35.075614, 138.497249 | Cape Jervis Formation, Upper Carboniferous-Lower Permian | 305-290 | 1.387 (2,183) | 2.387 (1,534) | 1.581 (1,016) | 39.6 (20) | 389.9±19.7 | 12.77±0.13 (122) | 1.41 | >130°C, 651-454 Ma<br>86-116°C, 498-320 Ma<br>63-76°C, 136-12 Ma |
| GC1069-67 | Hallett Cove | -35.074900, 138.495331 | Brachina Formation, Ediacaran | 609-590 | 1.388 (2,183) | 2.371 (649) | 2.513 (688) | 24.7 (20) | 252.2±15.6 | 12.12±0.16 (101) | 1.59 | >110°C, >300 Ma<br>91-103°C, 315-204 Ma<br>67-77°C, 56-6 Ma |
| GC1069-68 | Cape Jervis | -35.600870, 138.098260 | Cape Jervis Formation, Upper Carboniferous-Lower Permian | 305-290 | 1.388 (2,183) | 2.872 (1,171) | 2.246 (916) | 71.5 (20) | 339.5±17.8 | 11.61±0.22 (104) | 2.26 | >130°C, 582-443 Ma<br>95-100°C, 380-244 Ma<br>71-80°C, 73-8 Ma |
| GC1069-69 | Cape Jervis | -35.600789, 138.098188 | Carrickalinga Head Formation, Lower Cambrian | 522-514 | 1.388 (2,183) | 1.654 (942) | 1.696 (966) | 99.9 (20) | 260.6±14.1 | 12.23±0.15 (105) | 1.58 | >130°C, >307 Ma<br>92-103°C, 317-211 Ma<br>65-75°C, 50-0 Ma |
| GC1069-70 | Inman Valley | -35.496391, 138.512201 | Backstairs Passage Formation, Lower Cambrian | 522-514 | 1.389 (2,183) | 1.381 (662) | 1.416 (679) | 89.5 (20) | 260.7±16.1 | 11.94±0.20 (101) | 2.02 | >110°C, 504-317 Ma<br>90-100°C, 279-158 Ma<br>60-70°C, 78-0 Ma |
| GC1069-71 | Rosetta Head | -35.590222, 138.603407 | Encounter Bay Granite, Upper Cambrian | 515-506 | 1.389 (2,183) | 6.501 (1567) | 6.360 (1533) | 98.6 (20) | 273.1±12.5 | 11.89±0.15 (102) | 1.49 | >120°C, 372-322 Ma<br>83-94°C, 301-112 Ma<br>60-77°C, 47-0 Ma |
| GC545-2 | Sellicks Hill | -35.35937, 138.453032 | Mount Terrible Formation, Lower Cambrian | 529-526 | 1.356 (2,145) | 3.174 (821) | 3.476 (899) | 0.9 (20) | 238.6±18.3 | 12.56±0.14 (103) | 1.46 | >103°C, 334-248 Ma<br>71-78°C, 94-26 Ma |
| GC545-3 | Myponga Beach | -35.378386, 138.379933 | Sellick Hill Formation, Lower Cambrian | 525-524 | 1.357 (2,145) | 1.961 (654) | 1.910 (637) | 4.3 (20) | 271.7±20.2 | 12.61±0.15 (110) | 1.60 | 107-117°C, 364-264 Ma<br>65-74°C, 60-0 Ma |
| GC545-4 | Myponga Beach | -35.37205, 138.379183 | Sellick Hill Formation, Lower Cambrian | 525-524 | 1.358 (2,145) | 2.448 (644) | 2.247 (591) | 53.2 (20) | 284.4±18.1 | 12.61±0.14 (104) | 1.46 | >113°C, 370-298 Ma<br>64-77°C, 93-18 Ma |

**Table 1:** AFTA sample details and thermal history interpretation.